



UNIVERSIDADE DA BEIRA INTERIOR
Ciências

Understanding ion exchange chromatography adsorption mechanisms under different conditions

João Carlos Simões Cardoso

Dissertação para obtenção do Grau de Mestre em
Biotecnologia
(2º ciclo de estudos)

Orientador: Prof. Doutor Ana Cristina Mendes Dias-Cabral
Co-orientador: Mestre Gonçalo Fradique Lopes da Silva

Covilhã, junho de 2016

京まではまだ半空や雪の雲
*To the capital
Snow clouds forming,
half the sky to go*

Acknowledgments

Firstly, I would like to thank my supervisor Professor Cristina Dias-Cabral to be responsible for encouraging me and initiate me to the research world years ago. Her guidance, support and enthusiastic encouragement led me to follow my dreams with more passion and even made possible for me to, literally, adventure in the other side of the globe. A special thanks for her availability and concern.

I am particularly grateful for the assistance given by my co-supervisor Gonçalo Silva whom help and support were tirelessly. I really hope the opportunity to work with him in the future will rise.

I would also like to acknowledge my university UBI, research center CICS-UBI and colleagues, especially from my work group that are now close friends. Patrícia Aguilar, Filipa Pires, Gregory Dutra and Cláudia Peralta, I thank all the support, lunches, and the best un-related conversations.

A special thanks for my dear far away friends that help me unconditionally, Catarina Lima, Renato Guimarães, Lúcia Queiros, Carolina Batista, Cátia Costa and António Madeiras. Thank you for being part of my life.

And always, my whole family.

Resumo

Atualmente, a purificação de proteínas é tipicamente o aspecto mais dispendioso de um processo bio farmacêutico. A cromatografia de troca iônica (IEC), que se baseia na adsorção de proteínas numa resina ou suporte cromatográfico, é provavelmente o método mais utilizado na purificação destas proteínas devido a exibir uma grande capacidade de ligação para estas biomoléculas.

Ao investigar os diferentes eventos envolvidos na adsorção de proteínas desenvolve-se o conhecimento sobre o comportamento de proteínas em superfícies, o qual pode ser aplicado na purificação destas moléculas, bem como para uso em estudos biofísicos com base em fenómenos de reconhecimento molecular.

A microcalorimetria de fluxo (FMC) tem provado ser uma abordagem eficaz para medições de sinais de calor em tempo real, inerentes ao processo de adsorção que ocorre dentro de um sistema de cromatografia. Por conseguinte, permite uma melhor compreensão das forças que impulsionam o processo de adsorção.

O presente estudo tenta elucidar e comparar o mecanismo de adsorção de uma proteína modelo de alto peso molecular, soroalbumina bovina (BSA), em vários suportes cromatográficos de troca iônica disponíveis comercialmente, usando a técnica de FMC. Os suportes cromatográficos estudados carregados positivamente foram Toyopearl DEAE 650M, Toyopearl GigaCap Q-650M e TSKgel SuperQ 5PW. Sendo que a tecnologia de fixação de ligandos usada no seu fabrico difere. Além disso, por ser um suporte cromatográfico carregado negativamente e ter a mesma carga que a BSA nas condições em estudo, o TSKgel SP 5PW foi utilizado esperando uma interação primária mais fraca entre o suporte e a BSA. O estudo teve o objetivo de avaliar as diferenças termodinâmicas e foi uma tentativa para compreender forças mais fracas presentes no mecanismo de interação.

Os dados obtidos com uso de microcalorimetria de fluxo juntamente com as isotérmicas de adsorção ilustraram uma série de eventos cronológicos que ocorreram durante a adsorção da BSA nos suportes cromatográficos usados. Estes eventos incluíram: a libertação de moléculas de água e iões da superfície do suporte e da proteína; alterações conformacionais da proteína; “activated jump”; “chain delivery”; e desorção. Foi observado que estes eventos tiveram diferentes magnitudes quando se compararam os diferentes suportes cromatográficos de carga positiva, apesar de mostrarem o mesmo perfil de calor no termograma proveniente dos ensaios de FMC. Em condições de “não-ligação”, isto é, com ligandos do TSKgel SP 5PW e com a proteína ambos carregados negativamente, o perfil do termograma mudou

completamente. No entanto, na presença de 50 mM de cloreto de sódio, o comportamento dos perfis observados foi semelhante aos obtidos com os suportes cromatográficos de carga positiva.

Os estudos efetuados usando suportes cromatográficos carregados positivamente e TSKgel SP com a presença de 50 mM de cloreto de sódio mostraram entalpias de calor positivas aquando do contacto da proteína com o suporte. Assim, nestes casos, o mecanismo de adsorção foi considerado ser conduzido entropicamente, o que dá muito mais importância à troca de moléculas de água e iões neste complexo processo. Por outro lado, em ensaios onde o suporte TSKgel SP é usado na ausência de sal, o calor de adsorção total é negativo, o que significa que neste caso a adsorção é conduzida entalpicamente.

Palavras-chave

Microcalorimetria de fluxo, Seroalbumina bovina, mecanismo de adsorção, troca iónica

Resumo alargado

Atualmente, a purificação de proteínas é tipicamente o aspeto mais dispendioso de um processo bio farmacêutico.

Cromatografia de troca iónica (IEC), que se baseia na adsorção de proteínas numa resina ou suporte cromatográfico, é provavelmente o método mais utilizado na purificação destas proteínas devido a exibir uma grande capacidade de ligação para estas biomoléculas. A purificação de proteínas é altamente importante para o seu posterior uso terapêutico, e também como para estudos das suas funções e estrutura.

A adsorção de proteínas em qualquer superfície é um processo altamente complexo, e é controlado por vários subprocessos com efeitos sinérgicos e antagónicos provenientes de diferentes tipos de forças (Figure 1).

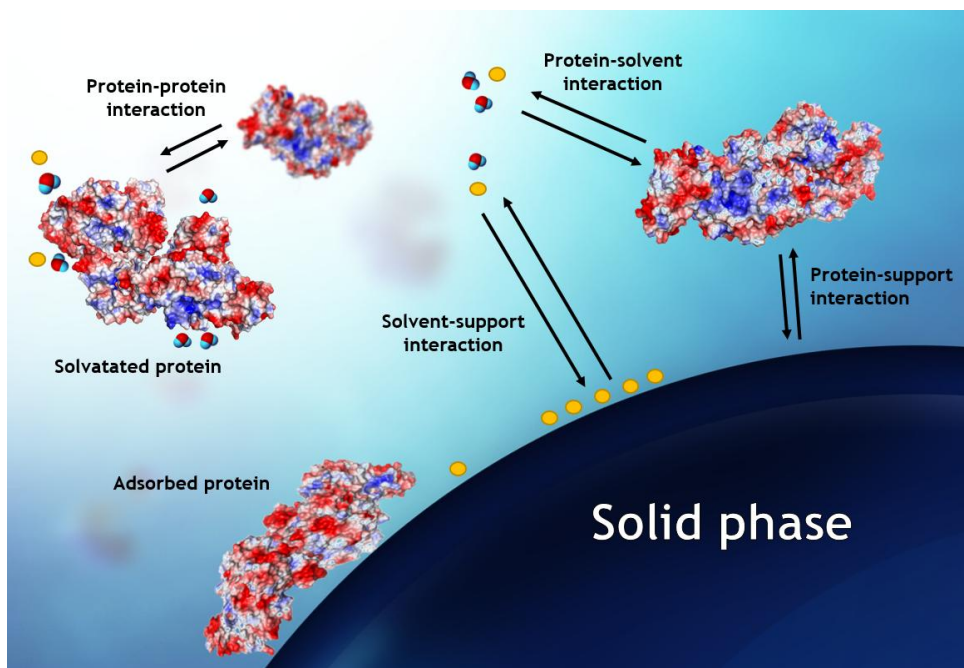


Figure 1 - Esquema simplificado das interações possivelmente envolvidas num mecanismo de adsorção de proteínas em suportes cromatográficos. Adaptado de ¹

Ao investigar os diferentes eventos envolvidos na adsorção de proteínas desenvolve-se o conhecimento sobre o comportamento de proteínas em superfícies que pode ser aplicado tanto na purificação destas moléculas, como também no desenvolvimento de estudos biofísicos com base em fenómenos de reconhecimento molecular.

A microcalorimetria de fluxo (FMC) tem provado ser uma abordagem eficaz para medições de sinais de calor em tempo real inerentes a processos de adsorção e desorção que ocorrem

dentro de um sistema cromatográfico. Por conseguinte, permite uma melhor compreensão das forças que impulsionam o processo de adsorção, sem interferir com as próprias moléculas e com o processo de adsorção.

O presente estudo tenta elucidar e comparar o mecanismo de adsorção de uma proteína modelo de alto peso molecular, seroalbumina bovina (BSA), em vários suportes cromatográficos de troca iónica disponíveis comercialmente usando a técnica de FMC. Os suportes cromatográficos estudados carregados positivamente foram Toyopearl DEAE 650M, Toyopearl GigaCap Q-650M e TSKgel SuperQ 5PW. Sendo que a tecnologia de fixação de ligandos usada no seu fabrico difere. Além disso, por ser um suporte cromatográfico carregado negativamente e ter a mesma carga que a BSA, nas condições em estudo, o TSKgel SP 5PW foi utilizado esperando uma interação primária mais fraca entre o suporte e a BSA. O estudo teve o objetivo de avaliar as diferenças termodinâmicas e foi uma tentativa para compreender forças mais fracas presentes no mecanismo de interação.

Os dados obtidos com uso de microcalorimetria de fluxo juntamente com as isotérmicas de adsorção ilustraram uma série de eventos cronológicos que ocorreram durante a adsorção da BSA nos suportes cromatográficos usados. Estes eventos incluíram: a libertação de moléculas de água e iões da superfície do suporte e da proteína; alterações conformacionais da proteína; “*activated jump*”; “*chain delivery*”; e desorção (Figure 2). Foi observado que estes eventos tiveram diferentes magnitudes quando se compararam os diferentes suportes cromatográficos de carga positiva, apesar de mostrarem o mesmo perfil de calor no termograma proveniente de ensaios de FMC.

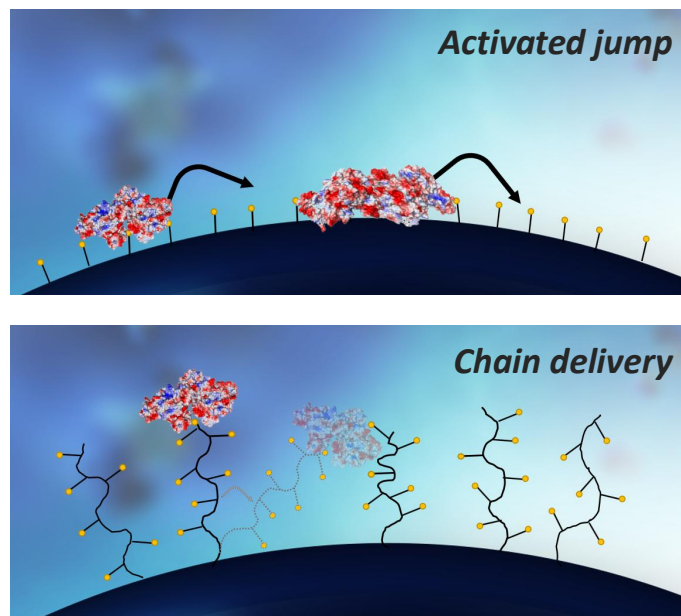


Figure 2 - Esquema de mecanismos de transporte presentes em suportes cromatográficos de troca iónica. (Cima) Mecanismo de “*activated jump*” presente em todos os suportes de troca iónica e (Baixo) mecanismo de “*chain delivery*” presente em suportes em cadeias com *grafting*. Adaptado de ²

E as alterações conformacionais da proteína parecem ser maiores quando os suportes cromatográficos possuem uma disposição bidimensional dos ligandos (sem “*grafting*”), devido a aumentarem a sua área de contacto após um espalhamento pela superfície.

Em condições de “não-ligação”, isto é, com ligandos do TSKgel SP 5PW e com proteína ambos carregados negativamente, o perfil do termograma mudou completamente. No entanto, na presença de 50 mM de cloreto de sódio, o comportamento dos perfis observados foi semelhante aos obtidos com os suportes cromatográficos de carga positiva.

Os estudos efetuados usando suportes cromatográficos carregados positivamente e TSKgel SP com a presença de 50 mM de cloreto de sódio mostraram apresentar entalpias positivas aquando do contacto da proteína com o suporte. Assim, o mecanismo de adsorção foi considerado ser conduzido devido a fatores entrópicos, o que dá muito mais importância à troca de moléculas de água e iões neste complexo processo. Por outro lado, ensaios com o suporte TSKgel SP na ausência de sal, o calor de adsorção total observado é negativo, o que significa que neste caso a adsorção é conduzida entalpicamente.

Tendo tudo em consideração, este trabalho consiste em mais um passo para a elucidação do complexo processo que é a adsorção de proteínas. Modelos teóricos, semi-empíricos e futuras simulações computacionais relacionadas com o mecanismo de adsorção, especialmente de moléculas com alto peso molecular, devem contabilizar os efeitos acima referidos, bem como as interações primárias. A combinação destas abordagens com investigações experimentais poderá futuramente conduzir para a possibilidade do desenvolvimento de suportes cromatográficos mais rápidos, eficazes e com melhores rendimentos. Com o objetivo final de simplificar e diminuir os custos associados à produção biotecnológica de biomoléculas com interesse farmacêutico.

Abstract

Nowadays, protein purification is typically the most laborious and more expensive aspect of a biopharmaceutical process. Ion exchange chromatography is probably the most used method in protein purification due to displaying the highest binding capacities for these biomolecules.

Protein adsorption onto any surface is a complex process that is controlled by a number of subprocesses with synergistic and antagonistic effects of different types of forces. Investigation of the events involved in protein adsorption promotes knowledge development on protein and surfaces behavior.

Flow microcalorimetry (FMC) has proven to be an effective approach to real-time heat signal measurements of adsorption and desorption events occurring inside a chromatographic system. Therefore, it allows a better understanding of the forces that drive the adsorption process without interfering with the system like the majority of used techniques.

The present study tries to elucidate and compare the mechanism of protein adsorption, namely bovine serum albumin, onto several commercially available charged resins using the FMC technique. The studied anion exchangers were Toyopearl DEAE 650M, Toyopearl GigaCap Q-650M, and TSKgel SuperQ 5PW. Being ligand attachment technology one of the differences between them. Also, although being a cation exchanger and having the same charge as BSA under the working conditions, TSKgel SP 5PW was used expecting a weaker primary interaction between BSA and the resin in order to evaluate the thermodynamic differences and to try to understand weaker forces of the inherited mechanism.

Flow microcalorimetry data coupled with equilibrium binding isotherms illustrated a series of chronological events that occurred during BSA adsorption onto the used resins, including resin and protein dehydration, protein conformational alterations, protein activated jump, chain delivery, and desorption. These events were found to have different magnitudes when comparing the anion exchangers in spite of showing the same heat profile.

In “non-binding conditions”, i.e., with TSKgel SP 5PW negative ligands and negative net protein charge, the thermogram profile completely changed. However, in the presence of 50 mM NaCl, the observed peak behavior was similar to those observed with anion exchangers.

The studied anion exchangers and TSKgel SP with 50 mM NaCl presented positive heat enthalpies when the protein was flowing through the FMC cell. Hence, the mechanism of adsorption was considered to be entropically driven, which gives much more importance to counter-ion and water molecules role in this complex process. On the other hand, with TSKgel

SP in the absence of salt, the adsorption net heat is negative, meaning that in this case adsorption is enthalpically driven.

All things considered, this work consisted on another step for the elucidation of the complex protein adsorption process. Theoretical, empirical models and future computational simulations of adsorption equilibrium should account for these complex effects, as well as the primary interactions.

Keywords

Flow microcalorimetry, Bovine serum albumin, adsorption mechanism, ion exchange.

Table of Contents

Chapter 1 - Introduction.....	1
1.1 Importance of protein purification	1
1.3 Protein adsorption process in liquid-solid chromatography	7
1.4 Interactions that contribute to protein adsorption	9
1.4.1 Hydrogen bond	9
1.4.2 Hydrophobic Interaction	10
1.4.3 Electrostatic Interaction.....	11
1.4.4 Van der Waals interactions.....	12
1.4.5 Coordination Bond	12
1.4.6 Conformational Entropy	12
1.5 Protein surface, orientation and conformational role in adsorption	13
1.6 Subprocesses of protein adsorption	15
1.7 Thermodynamic aspects of interaction in chromatography.....	17
1.7.1 Processes that can contribute to enthalpy and entropy change in IEC protein adsorption	17
1.7.2 Van't Hoff plot analysis.....	20
1.7.3 Microcalorimetry techniques.....	20
1.7.3.1 Isothermal titration calorimetry.....	21
1.7.3.2 Flow microcalorimetry	21
1.8 Theoretical aspects of adsorption mechanism in preparative chromatography	24
1.8.1 Langmuir model	24
1.8.2 Steric mass action model	25
1.8.3 Potential barrier chromatography theory and electrical double layer	26
Chapter 2 - Goal of the study.....	31
Chapter 3 - Materials and Methods	33
3.1 Adsorption isotherm measurements	33
3.2 Flow microcalorimetry	34
Chapter 4 - Results and Discussion.....	35
4.1 Resins structural differences	35

4.2 Adsorption isotherms data	36
4.3 Microcalorimetric data	38
4.3.1 First endothermic peak	40
4.3.2 Second endothermic peak	42
4.3.3 Exothermic peak	43
4.3.4 “Non-binding” conditions data	46
4.4 Adsorption driving forces.....	50
Chapter 5 - Conclusions.....	51
References	53
Appendix I.....	59

List of figures

Figure 1 - Esquema simplificado das interações possivelmente envolvidas num mecanismo de adsorção de proteínas em suportes cromatográficos. Adaptado de ¹	ix
Figure 2 - Esquema de mecanismos de transporte presentes em suportes cromatográficos de troca iónica. (Cima) Mecanismo de “activated jump” presente em todos os suportes de troca iónica e (Baixo) mecanismo de “chain delivery” presente em suportes em cadeias com grafting. Adaptado de ²	x
Figure 3 - Schematics of a conventional column chromatography (A) and continuous annular chromatography (B) mostly used in biotechnological industries. The process is two dimensional in both cases. Adapted from ⁶	2
Figure 4 - Qualitative electrostatic representation of bovine serum albumin (BSA) charged surface. The heterogeneity of charges in this asymmetrical protein is clearly shown. BSA heterogeneous surface is shown on the lower panel and colored according to the electrostatic potential calculated with PyMOL ¹⁷ molecular graphics software ignoring solvent screening effect. For electrostatic potential, red is used for negative (-) and blue for positive (+).....	5
Figure 5 - Simplified scheme of liquid-solid equilibrium interactions in a chromatography system. Adapted from ¹	7
Figure 6 - Example of a hydrogen bond between water and ammonia molecules. ($\delta+$) represents positive partial charges and ($\delta-$) represents negative partial charges due to atom electronegativity ³³	9
Figure 7 - Scheme of hydrophobic interactions and reorganization of water molecules. Note that the number of ordered water molecules decrease after the interaction, which makes this process entropically favorable.	10
Figure 8 - Schematic representation of the oriented alignment of proteins induced by like-charged surfaces. The oriented alignment maximizes the electrostatic repulsions, leading to the inhibition of protein aggregation. Adapted from ²	11
Figure 9 - Schematic diagram of chicken egg white lysozyme (CEWL) orientation at chromatographic surfaces at pH 7. CEWL heterogeneous surface is shown on the left panel and colored according to the lipophilic potential or the electrostatic potential. For lipophilic potential, brown is used for hydrophobic (H) and blue for hydrophilic (P). For electrostatic potential, red is used for positive (+) and purple for negative (-). Adapted from ²	13
Figure 10 - Examples of two van't Hoff plots for two types of reactions. This linear behavior is rarely observed when studying biomolecules.	20
Figure 11 - Schematics of a flow microcalorimetry system and all its constituents.	22
Figure 12 - Example of a characteristic thermogram showing an electrical pulse given to the system (calibration peak) followed by an endothermic and exothermic events. Represented with consent of the author ⁷⁰	23

Figure 13 - Adsorption equilibrium isotherm example. Obtained plotting surface concentration of a given molecule versus the concentration obtained after the equilibrium. 25

Figure 14 - Electrical double layer scheme of a positively charged molecule. Negative ions are represented in red and positive charged ions are represented as blue. 27

Figure 15 - Interaction Potential energy profiles relevant to potential barrier chromatography. Red line represents the total interaction potential with the location of the maximum, \emptyset_{\max} , and minimum, \emptyset_{\min} , of the interaction potential energy profiles associated with the adsorption energy well and the potential barrier respectively. Adapted from ¹⁸. 28

Figure 16 - Flow microcalorimeter used in the experiments of this work at CICS-UBI. 34

Figure 17 - Equilibrium binding isotherms for bovine serum albumin adsorption onto ion exchange resins at Tris-HCl pH 9 and 295 K. (●) TSKgel SuperQ 5PW, (◆) Toyopearl DEAE 650M, (▲) Toyopearl GigaCap Q-650M (■) TSKgel SP 5PW. 36

Figure 18 - FMC thermogram obtained for 230 μL injection of 50 $\text{mg}\cdot\text{mL}^{-1}$ BSA in equilibrium buffer Tris-HCl pH 9 adsorbing onto (●) TSKgel SuperQ 5PW, (◆) Toyopearl DEAE 650M and (▲) Toyopearl GigaCap Q-650M. Surface concentration (and flowthrough %) are respectively, 21.5 $\text{mg}\cdot\text{mL}^{-1}$ resin (66 %), 27.66 $\text{mg}\cdot\text{mL}^{-1}$ resin (52%) and 23.28 $\text{mg}\cdot\text{mL}^{-1}$ resin (61%). Shaded area represents the interval of time at which the protein plug contacts with the support. 38

Figure 19 - PEAKFIT deconvolution of thermogram for BSA adsorption onto TSKgel SuperQ 5PW with Tris-HCl pH 9 for 230 μL injection of 50 $\text{mg}\cdot\text{mL}^{-1}$ resulting in surface concentration of 8.37 $\text{mg}\cdot\text{mL}^{-1}$ resin. Shaded area represents the interval of time at which protein flowed through the cell. 39

Figure 20 - First endothermic peak area related with surface concentration obtained for 230 μL injections of BSA in Tris-HCl pH 9 adsorbing onto (●) TSKgel SuperQ 5PW, (◆) Toyopearl DEAE 650M and (▲) Toyopearl GigaCap Q-650M. First endothermic peaks obtained for 30 μL injections of the same solutions onto (●) TSKgel SuperQ 5PW are also shown. Only considered trials with a linear relation between injection concentration and surface concentration were considered. 40

Figure 21 - Second endothermic peak area related with surface concentration obtained for 230 μL injections of BSA in Tris-HCl pH 9 adsorbing onto (●) TSKgel SuperQ 5PW, (◆) Toyopearl DEAE 650M and (▲) Toyopearl GigaCap Q-650M. Second endothermic peaks obtained for 30 μL injections of the same solutions onto (●) TSKgel SuperQ 5PW are also shown. Only considered trials with a linear relation between injection concentration and surface concentration were considered. 42

Figure 22 - Exothermic peak area related with flowthrough obtained for 230 μL injections of BSA in Tris-HCl pH 9 adsorbing onto (●) TSKgel SuperQ 5PW, (◆) Toyopearl DEAE 650M and (▲) Toyopearl GigaCap Q-650M. Note that TSKgel SuperQ 5PW thermogram with no flowthrough (●) was obtained with a 30 μL loop. The smaller graph in the left bottom corner is a zoom in of lower flowthrough percentages. 43

Figure 23 - Schematics of surface transport mechanisms present in IEC resins. (Top) Activated jump present in all IEC resins and (Bottom) Chain delivery mechanism present in grafted resins, for example: TSKgel SuperQ and Toyopearl GigaCap. Adapted from ²	44
Figure 24 - Exothermic peak area related with surface concentration obtained with 30 μ L injections of BSA in Tris-HCl pH 9 adsorbing onto TSKgel SuperQ 5PW. Obtained with no flowthrough.	45
Figure 25 - FMC thermograms obtained for 230 μ L injection of different concentrations of negatively net charged BSA in equilibrium buffer Tris-HCl pH 9 adsorbing onto negatively charged TSKgel SP 5PW. Surface concentrations are respectively (green) 2.8 mg.mL ⁻¹ , (dark blue) 5.85 mg.mL ⁻¹ , (grey) 30.03 mg.mL ⁻¹ , (orange) 45.71 mg.mL ⁻¹ and (light blue) 65.0 mg.mL ⁻¹ . Shaded area represents the interval of time at which there was protein flowing through the cell.	46
Figure 26 - Exothermic peak area related with BSA surface concentration. Obtained with TSKgel SP 5PW with 230 μ L injections with Tris HCl pH 9.	47
Figure 27 - FMC thermograms obtained for 230 μ L injection of BSA in 20 mM Tris-HCl at pH 9 with 50 mM NaCl adsorbing onto TSKgel SP 5PW with the respective surface concentration obtained. The shaded area corresponds to the protein plug in the cell.	48
Figure 28 - Equilibrium binding isotherm for BSA adsorption onto TSKgel SP 5PW in Tris-HCl pH 9 with 20 mM Tris at 295 K in the absence of salt (●) and with 50 mM NaCl (◆).	49
Figure 29 - FMC thermograms obtained for 230 μ L injection of different BSA solutions concentrations in equilibrium buffer Tris-HCl pH 9 adsorbing onto TSKgel SuperQ 5PW. Injection concentrations are represented in the figure followed by the resulting surface concentration obtained. For example: (dark blue) thermogram was obtained injecting 50 mg.mL ⁻¹ BSA solution resulting in 21.5 mg BSA.mL ⁻¹ TSKgel SuperQ.....	59
Figure 30 - FMC thermograms obtained for 230 μ L injection of different BSA solutions concentrations in equilibrium buffer Tris-HCl pH 9 adsorbing onto Toyopearl DEAE 650M. Injection concentrations are represented in the figure followed by the resulting surface concentration obtained. For example: (light green) thermogram was obtained injecting 20 mg.mL ⁻¹ BSA solution resulting in 22.16 mg BSA.mL ⁻¹ Toyopearl DEAE.....	60
Figure 31 - FMC thermograms obtained for 230 μ L injection of different BSA solutions concentrations in equilibrium buffer Tris-HCl pH 9 adsorbing onto Toyopearl GigaCap Q-650M. Injection concentrations are represented in the figure followed by the resulting surface concentration obtained. For example: (dark blue) thermogram was obtained injecting 75 mg.mL ⁻¹ BSA solution resulting in 74.9 mg BSA.mL ⁻¹ Toyopearl GigaCap Q-650M.	61

List of tables

Table 1 - Branches of liquid chromatography based on stationary phase ligand and mobile phase proprieties. Adapted from ⁶	4
Table 2 - List of most used ion-exchange ligands on current chromatographic systems and its structure. Adapted from ¹⁵	4
Table 3 Charge of the ligand on different values of solution pH. Adapted from ¹⁶	5
Table 4 - Post-translational modifications contributing to charge properties and charge alterations of proteins. Adapted from ¹²	6
Table 5 - Bovine serum albumin physical isomers physical parameters. Adapted from ³⁰	14
Table 6 - Summary of events responsible for thermodynamic changes in a chromatographic system. Note that some of these events are interconnected and all are highly related.	19
Table 7 - Expected signs of the enthalpic processes based in upon a large body of thermodynamic results for protein-ligand association in solution and protein-solid phase interaction. Adapted from Ross et al. ³⁹	19
Table 8 - Structural parameters of the studied resins together with the observed static binding capacity and affinity constants calculated from Langmuir linearized equation.....	35

Chapter 1 - Introduction

1.1 Importance of protein purification

Proteins are complex molecules composed of amino acids. These have the most dynamic and diverse roles than any other macromolecule in the animal body. Some of their functions include: catalysis of biochemical reactions; formation of receptors and channels in membranes; giving intracellular and extracellular scaffolding support; and transportation of molecules within a cell or from one organ to another ³. Formerly, protein therapeutics was a rarely used subset of medical treatments. Nevertheless, its application has increased dramatically since the introduction of the first recombinant protein, human insulin, 35 years ago ⁴. Recombinant proteins are produced through recombinant deoxyribonucleic acid (DNA) technology, which involves inserting the protein encoding DNA into bacterial, yeast, vegetal, insect or mammalian cells, expressing the protein in these cells and then purifying the protein of interest from them. Many biological medical products such as monoclonal antibodies and biosynthetic human insulin are examples of recombinant protein therapies ⁵. Purified proteins are used in disease treatments in which have several advantages over small-molecule drugs ³, such as:

- High specific and complex set of functions that chemical compounds cannot mimic.
- Less potential for protein-based therapies interfere with normal biological processes and cause adverse effects due to the fact that proteins are highly specific.
- Replacement treatment in diseases that have a mutated gene. Since gene therapy is not currently available for most genetic disorders.

Molecules used in recombinant protein therapies are required to have a very high degree of purity. This purification process is also vital for studies of the function, structure and interactions of the protein of interest. There are several steps involved in the acquisition of a specific purified protein from a mixture. These steps may separate the protein from non-protein parts of the mixture in a prior stage, and finally separate the chosen protein from all other proteins with a desired purity. Separation of one protein from others is typically the most laborious aspect of protein purification ⁶. This or these separation steps may be accomplished with liquid chromatography due to its proven efficiency, specificity and the lack of better techniques. Liquid chromatography technique can exploit differences in protein size, physico-chemical properties, binding affinity and biological activity.

1.2 Liquid-solid chromatography contemporary viewpoint

Liquid-solid chromatography (LC) is a process that employs a fixed-bed of a solute-interacting material, known as the stationary phase, to separate a mixture of components that are carried by a fluid phase, known as the mobile phase. Liquid-solid chromatography includes a variety of interaction mechanisms and modes of operation for the separation of mixtures, but in all cases the mixture of components that are to be separated must interact differently with the stationary phase and the mobile phase. Figure 3 shows a scheme of a conventional column liquid chromatography (A) and a continuous annular chromatography (B) currently used in laboratories and in some industries ⁶.

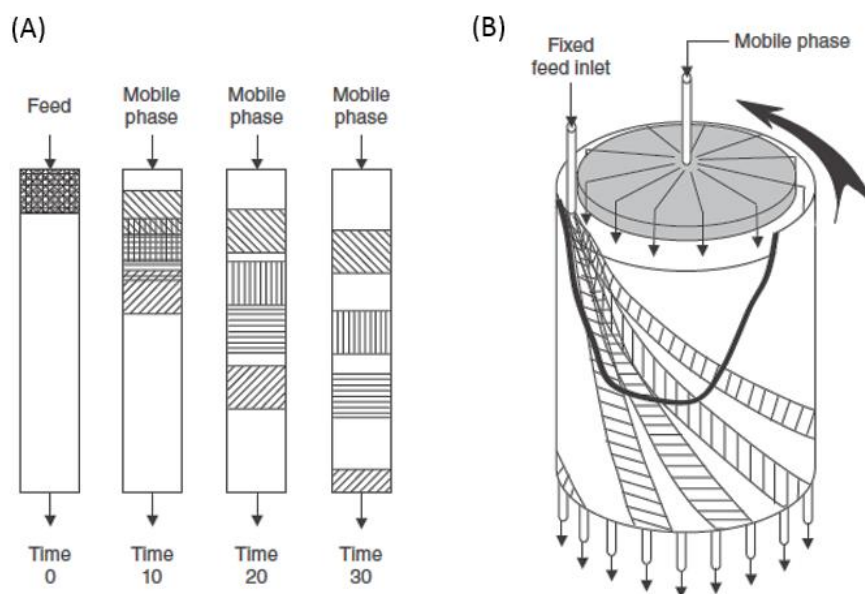


Figure 3 - Schematics of a conventional column chromatography (A) and continuous annular chromatography (B) mostly used in biotechnological industries. The process is two dimensional in both cases. Adapted from ⁶.

The purpose of chromatography is not always purification, it can be also used for analytical applications:

- In preparative chromatography the objective is to obtain one isolated pure substance for posterior use ⁷.
- In analytical chromatography the main objective is the separation of molecules with the final objective of analysis, quantification, identification ⁸ as well as studies of the protein's structure ⁹, post-translational modifications ¹⁰ and function ^{9,11};

The present work will focus only in preparative chromatography.

Contemporary liquid-solid chromatography can be divided, based on the type of stationary phase ligate nature, into several branches (summarized Table 1).

Size exclusion chromatography (SEC) is grounded on non-adsorptive phenomena of proteins enabling separation of molecules based on the difference in its retention factors dependent on the molecule size ¹².

Reversed phase chromatography (RPC) uses hydrophobic ligands that bind strongly with hydrophobic molecules or moieties in proteins ⁶. The elution is mainly performed with water-miscible organic solvents, which have non-polar characteristics in order to reduce protein interaction with the stationary phase. Unfortunately, that may cause protein denaturation due to high hydrophobicity, leading to the usually irreversible exposure of hydrophobic moieties that are in the interior of the globular protein. This is one of the major disadvantages of this type of stationary phases used in preparative chromatography. However, RPC is very popular for chromatographic analytical purposes ^{6,12}.

Another branch based on hydrophobic ligands is hydrophobic interaction chromatography (HIC). The hydrophobic ligands are presumed to interact with hydrophobic side chains of the protein. The hydrophobic character of a protein is promoted in presence of anti-chaotropic salts. The salt changes the hydration shell of both, the protein and the ligand, which promotes hydrophobic interaction forces (the so called salting out effect). Salt may also in some cases alter the conformational structure of proteins ¹². The elution in HIC is achieved by decreasing salt concentrations instead of using organic solvents, which makes this approach much more attractive to preparative chromatography.

Ligands that have the ability to recognize one of the structural motifs of a molecule are used in what is called biospecific or affinity chromatography. This interaction can be extremely specific and the ligand will interact with only one type of molecule, or the ligand can be designed so that it recognizes a group of structurally similar molecules. Nevertheless, if the adsorption is too strong it will make it too difficult to desorb the target protein from the column.

Ion exchange chromatography (IEC) is probably the most used liquid chromatographic method in protein purification due to displaying the highest binding capacities for these biomolecules¹³. It was indicated that about 40% of chromatographic steps for protein purification are IEC, on an average of three chromatographic steps in the process¹⁴. IEC is based on the binding of proteins to charged groups immobilized on the solid phase which are in equilibrium with free counter-ions in the mobile phase. Table 2 and Table 3 refer the present-day most common ligands used in IEC.

Table 1 - Branches of liquid chromatography based on stationary phase ligand and mobile phase proprieties. Adapted from⁶.

<i>Stationary phase ligate</i>	<i>Mobile phase</i>	<i>Branch</i>	<i>Acronym</i>
None	Aqueous	Size exclusion	SEC
Hydrophobic	Normally a water-organic solvent mixture. Elution with increasing percentage of organic solvent.	Reversed phase	RPC
Mildly hydrophobic	Normally an aqueous solution with high anti-chaotropic salt concentration. Elution with decreasing salt concentrations	Hydrophobic interaction	HIC
Charged	Normally an aqueous solution with low salt concentration. Elution by increasing salt concentrations	Ion exchange	IEC
Biospecific	Aqueous. Elution varies with the system	Affinity/biospecific interaction	AC/BIC

Table 2 - List of most used ion-exchange ligands on current chromatographic systems and its structure. Adapted from¹⁵.

<i>Ligand name</i>	<i>Acronym</i>	<i>Structure of ligand</i>	<i>Strength</i>
Quaternary ammonium	Q	$-O-CH_2N^+(CH_3)_3$	Strong anion exchanger
Diethylaminoethyl	DEAE	$-O-CH_2CH_2NH(CH_2CH_3)_2$	Weak anion exchanger
Carboxymethyl	CM	$-O-CH_2COO^-$	Weak cation exchanger
Sulfopropyl	SP	$-O-CH_2CHOHCH_2OCH_2CH_2CH_2SO_3^-$	Strong cation exchanger
Methyl sulfonate	S	$-O-CH_2CHOHCH_2OCH_2CHOHCH_2SO_3^-$	Strong cation exchanger

Table 3 Charge of the ligand on different values of solution pH. Adapted from ¹⁶.

Ligand	Acronym	Charge of the ligand dependent on the solution pH						
		<2	2-2.5	2.5-3	3-5	5-7	7-10	10-11
Quaternary ammonium	Q	Z = +1						Not stable
Diethylaminoethyl	DEAE	Z = +1			0 < Z < 1		Z = 0	
Carboxymethyl	CM	Z = 0		-1 < Z < 0		Z = -1		
Sulfopropyl	SP	Z = 0		Z = -1				
Methyl sulfonate	S	Z = 0		Z = -1				

In this process of adsorption the counter-ions are *exchanged* with the charged protein, hence the name ion exchange chromatography. Charged amino acid residues located in the protein surface and other several types of surface modifications that alter the surface charge properties (namely charged groups which are post-translationally attached to proteins) are believed to be responsible for the adsorption process ¹², see Figure 4. Some post-translation modifications that contribute greatly for the protein surface charge are shown in Table 4 as an example.

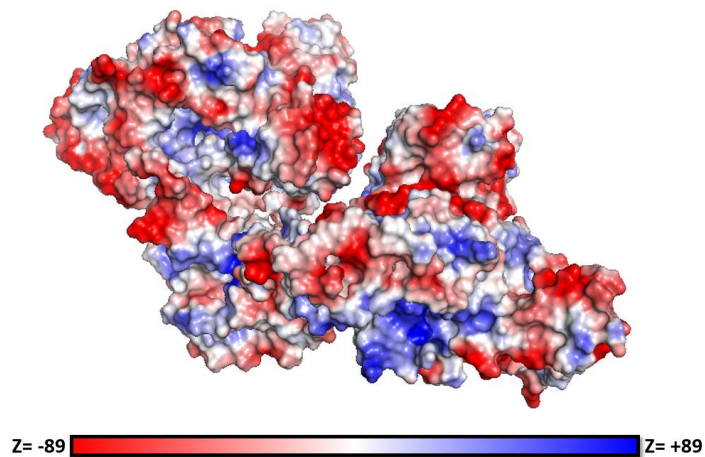


Figure 4 - Qualitative electrostatic representation of bovine serum albumin (BSA) charged surface. The heterogeneity of charges in this asymmetrical protein is clearly shown. BSA heterogeneous surface is shown on the lower panel and colored according to the electrostatic potential calculated with PyMOL¹⁷ molecular graphics software ignoring solvent screening effect. For electrostatic potential, red is used for negative (-) and blue for positive (+).

Table 4 - Post-translational modifications contributing to charge properties and charge alterations of proteins. Adapted from ¹².

<i>Residue in which alteration occurs</i>	<i>Functional Group</i>	<i>pK</i>	<i>Post-translational modifications which alter the charge proprieties</i>	
Alterations of charged functional groups	Aspartic Acid	Carboxylate	4.5	Phosphate group addition
	Tyrosine	Phenolic hydroxyl	9.7	O-sulfate. O-5'-adenylate, O-phosphate
	Cysteine	Thiol	9.3	S-glucosyl, S-galactosyl, S-phosphate
	Lysine	Amino	10.4	N-methyl (mono, di), N-acetyl, N-ADP-ribosyl
	Arginine	Guanidino	12	ω -N-methyl (mono, di), N-ADP-ribosyl.
	Histidine	Imidazol	6.2	N(3)-phosphate
	α -Amino	Amino	6.8-7.9	N-acetyl, N-myristoyl, Schiff base with carbohydrates
	α -Carboxyl	Carboxylate	3.5-4.3	Methylation after S-farmesylation of subterminal cysteine, glycosyl-phosatidylinositol via phosphor-ethanolamine.
Introduction of charged functional groups	Glutamic Acid	Carboxylate	4.6	γ -Carboxylate
	Serine	Hydroxyl	n.a.	O-phosphate, Sialoglycosyl
	Threonine	Hydroxyl	n.a.	O-phosphate, Sialoglycosyl
	Asparagine	Carboxamide	n.a.	Sialoglycosyl
	5-Hydroxylysine	Hydroxyl	n.a.	Sialoglycosyl
	4-Hydroxyproline	Hydroxyl	n.a.	Sialoglycosyl

1.3 Protein adsorption process in liquid-solid chromatography

In liquid-solid chromatography, the stationary phase should have the ability to attract the target substances by what may be considered as a dynamic equilibrium. This equilibrium is very complex and Figure 5 represents an over-simplified model scheme of the adsorption mechanism in general chromatography systems. In this model there is an equilibrium where molecules of the mobile phase, or ions and water molecules in ion exchange chromatography, are continually being adsorbed and desorbed from the stationary phase. When the protein or mixture is introduced the equilibrium conditions between the mobile phase and the adsorbed surface are disturbed, creating a competition for the adsorptive sites on the surface of the chromatographic support. A stronger affinity between the support and the protein will lead to more displacement of solvent molecules/ions in favor of the protein molecules. It must be considered that this scheme is too elementary to represent all the interactions that occur in a chromatographic system. There are additional interactions between the proteins themselves and mobile phase molecules/ions that also interact with proteins, this will be covered into deeper detail later in this work. The magnitude of interaction of a protein with a surface is governed by the system free energy before and after the interaction and can be attributed to changes in system enthalpy and entropy¹⁸.

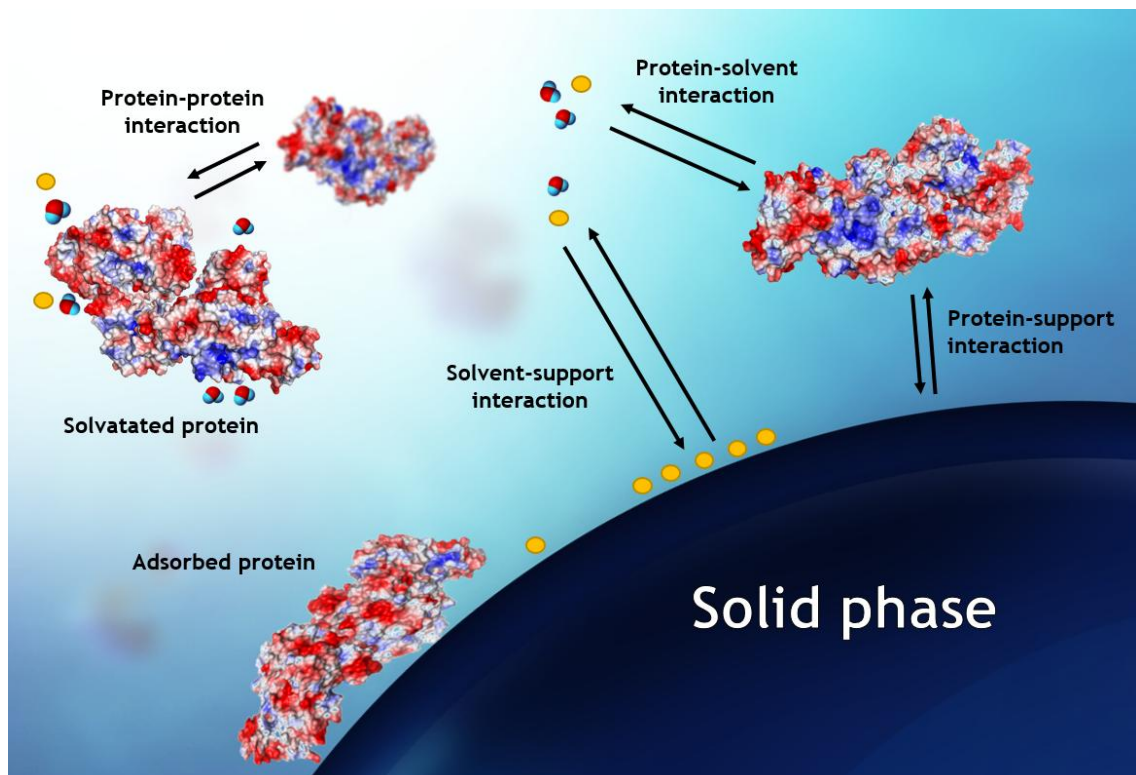


Figure 5 - Simplified scheme of liquid-solid equilibrium interactions in a chromatography system. Adapted from¹

For effective protein retention to occur, the choice of mobile phase must be such that protein molecules have higher attraction towards the adsorbent than mobile phase molecules. However, the affinity should not be too strong not to hinder the elution of the target protein in the elution buffer ¹.

This equilibrium is established under static conditions when the mobile phase is not in motion and defines the equilibrium binding capacity (EBC). Under dynamic conditions, i.e., when the mobile phase is flowing through the column, dynamic binding capacity (DBC) dictates packed columns performance, the DBC is generally related to EBC but is influenced by dispersive factors, approaching the EBC only for conditions where the column has infinite efficiency ^{1,6}.

Given these points, it is clear the necessity to understand and further elucidate these complex interactions that contribute to protein adsorption phenomena.

1.4 Interactions that contribute to protein adsorption

Some of the technological problems regarding the mechanism of adsorption and aggregation are being studied by using computational molecular simulations¹⁹⁻²⁶ combined with theoretical^{27,28} and experimental investigations^{2,29-31}. As explained before, protein adsorption at chromatographic surfaces involves various interactions between the protein and surface or the ligands attached to the surface. The interactions that contribute to protein adsorption may include, hydrogen bonding, hydrophobic interaction, electrostatic interaction, van der Waals interaction, coordination bonding and conformational entropy among others, resulting from the interplay between them¹⁵.

1.4.1 Hydrogen bond

A hydrogen bond is an interaction in which a hydrogen atom is attracted simultaneously by two electronegative atoms. Hydrogen bonding energy decreases with increasing temperature and ion strength¹⁵, as well as by the presence of chaotropic agents such as urea and guanidine hydrochloride. According to Norde, contributions from hydrogen bonding (other than accounted for in the hydrophobic effect) are believed to have only a minor effect on protein adsorption³².

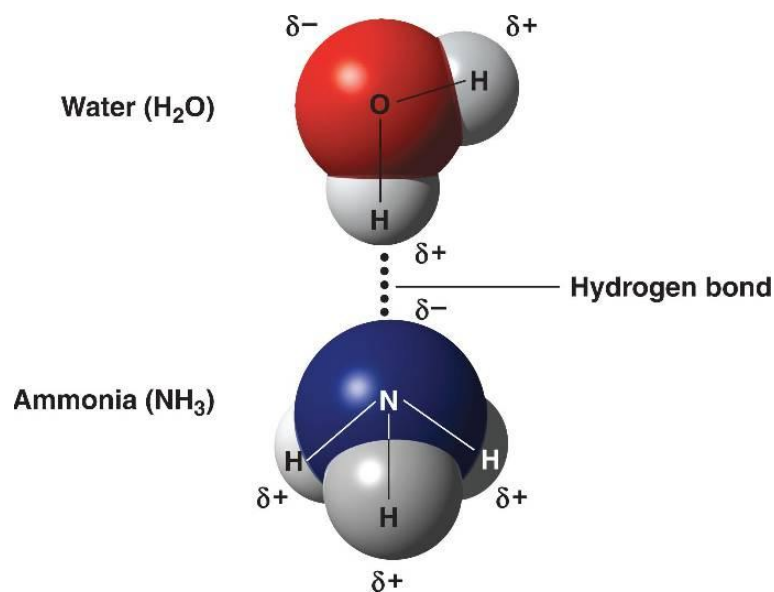


Figure 6 - Example of a hydrogen bond between water and ammonia molecules. (δ^+) represents positive partial charges and (δ^-) represents negative partial charges due to atom electronegativity³³.

1.4.2 Hydrophobic Interaction

A solute or moiety is considered hydrophobic if it binds to water more weakly than water itself³⁴. Hydrophobic interaction is caused by redistribution of ordered water molecules around apolar moieties back into bulk solution that causes the association of apolar parts, as shown in Figure 7. This association can be between protein-protein hydrophobic patches or protein-support hydrophobic interaction¹⁵. It has been estimated that dehydration of hydrophobic surfaces results in a reduction in the Gibbs energy of $5\text{-}15\text{ mJ}\cdot\text{m}^{-2}$ ³². This is mainly due to entropy increase because water molecules get released from the surface of the protein or the solid phase.

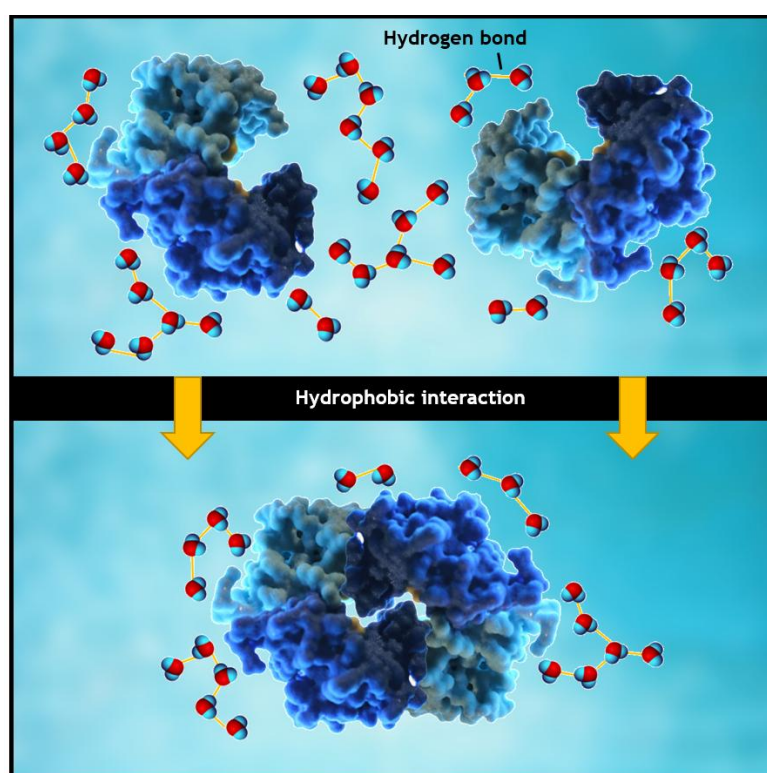


Figure 7 - Scheme of hydrophobic interactions and reorganization of water molecules. Note that the number of ordered water molecules decreases after the interaction, which makes this process entropically favorable.

Increasing temperature and/or salt concentration usually causes stronger hydrophobic interactions. It is known that water molecules have a higher tendency for hydration of the salt molecules than macromolecules and consequently the presence of the salt can enhance the hydrophobic interaction because it will reduce the number of water molecules that are surrounding the proteins³⁵, promoting protein adsorption. Salt type also changes the magnitude of these forces. Anti-chaotropic or kosmotropic salts promotes hydrophobic interactions⁶.

1.4.3 Electrostatic Interaction

Electrostatic phenomena arise from the forces that electric charges exert on each other. Such forces are described by Coulomb's law.

Figure 8 shows a representation of these forces inside a chromatographic support pore. Basically, opposite charges attract and similar ones repel each other. When the molecule and the stationary surface are both charged, electrostatic interaction, attractive or repulsive, can occur between them.

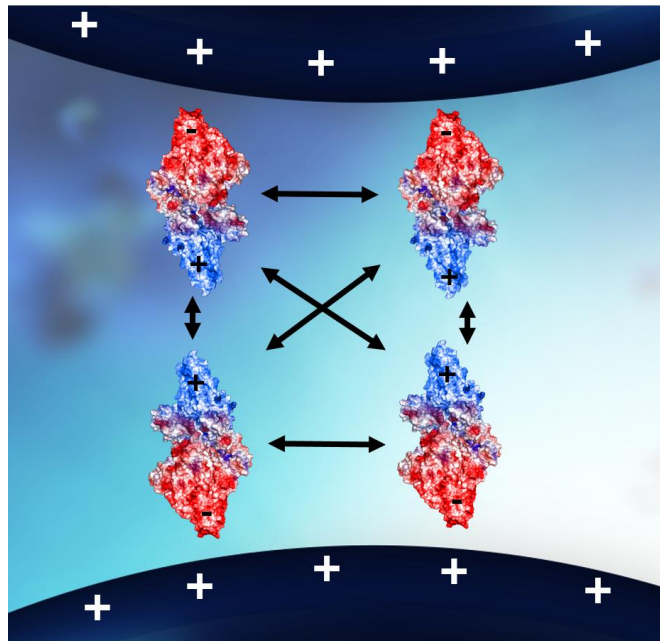


Figure 8 - Schematic representation of the oriented alignment of proteins induced by like-charged surfaces. The oriented alignment maximizes the electrostatic repulsions, leading to the inhibition of protein aggregation. Adapted from ².

The strength of electrostatic interaction depends on the charge numbers, so it is significantly affected by both pH and ionic strength. The increase of ionic strength will weaken (screen) or even completely shield the electrostatic interaction. The increase of temperature reduces electrostatic effect due to the enhanced thermal motion of molecules and atoms at elevated temperature ¹⁵. These forces are also responsible for inhibiting aggregation and refolding of a protein inside a chromatography column ².

1.4.4 Van der Waals interactions

Van der Waals interactions are relatively weak forces of attraction between electrically neutral molecules that collide with or pass very close to each other. There are still some contradictions in this area, some authors state that van der Waals interactions hardly influence adsorption of proteins³² but newer studies showed that van der Waals forces may even be the driving force of protein adsorption in chromatographic supports, especially in the presence of salt^{18,36,37}. These forces have a very limited range of distance (around 0.2 nm)¹⁵. Due to their short range they need the occurrence of previous events, water molecule displacement due to hydrophobic interaction is one example. For that reason, van der Waals forces are often considered the major contribution to the hydrophobic interaction³⁸.

However, van der Waals forces are believed to be weaker than most of the other molecular interactions, usually releasing energy in the order of -6.56×10^{-6} to -0.03 J.m^{-2} , without salt and with salt respectively^{36,39}

1.4.5 Coordination Bond

These interactions occur between solid phase metal ions, such as Cu^{2+} , Zn^{2+} , Ni^{2+} , and Co^{2+} and imidazole group of histidine amino acid from the proteins. It is very specific and can be weakened with increasing temperature or the presence of chelating agents, e.g., ethylenediaminetetraacetic acid (EDTA) due to binding possibility with metal ions¹⁵.

1.4.6 Conformational Entropy

Adsorption results in the reduction of conformational entropy, so conformational entropy is thermodynamically unfavorable for adsorption¹⁵. Therefore, adsorption takes place only if the loss in conformational entropy is compensated by sufficient attraction between the solute molecules and the surface or the entropy gained with the release of water molecules to the bulk solution. This process will be further elucidated in this work.

In summary, protein adsorption is a complex process that is controlled by a number of subprocesses with synergistic and antagonistic effects of the interactions mentioned above. These subprocesses of adsorption will be further explained in this chapter. Examinations of the interactions involved in protein adsorption facilitate the knowledge development and findings on protein behavior at chromatographic surfaces. Furthermore, knowledge on the binding behavior of proteins may also provide valuable insight into the molecular mechanisms of protein-protein or protein-membrane interactions in a biological context¹⁸.

1.5 Protein surface, orientation and conformational role in adsorption

The diversity of the amino acids hydrophobicity/hydrophilicity or charged/neutral features results in an extraordinary structural complexity of protein molecules. Things become more complex when considering the folding of protein molecules into their secondary and tertiary structures⁴⁰.

Protein folding leads to a heterogeneous surface that can be decomposed into individual patches exhibiting specific properties. Bovine serum albumin (BSA), for example, consists of three domains that repeat the α -helix pattern. The BSA molecule is characterized by an asymmetric charge distribution. Considering the theoretical calculations, domains I, II and III have charges -9 , -7.8 and -1.3 , respectively, at pH 7.0³⁰. Its isoelectric point (pI) is reported on a pH range from 4.8 to 5.6⁴¹. Protein behavior at chromatographic surfaces is complex, often results of interplay of attraction and repulsion of individual patches on the heterogeneous surface of protein that have diverse properties. At a positively charged surface, negative charged patches of the protein molecule are attracted and tend to bind to the surface while the positively charged patches are repulsed away from the surface, see Figure 9. Similarly, hydrophobic patches of the protein molecule are attracted to a hydrophobic surface while the hydrophilic patches are repulsed, due to water molecules movement. Rotation of the protein molecule or conformational alterations are then driven by attraction and/or repulsion, leading to preferred binding sites on protein⁴⁰.

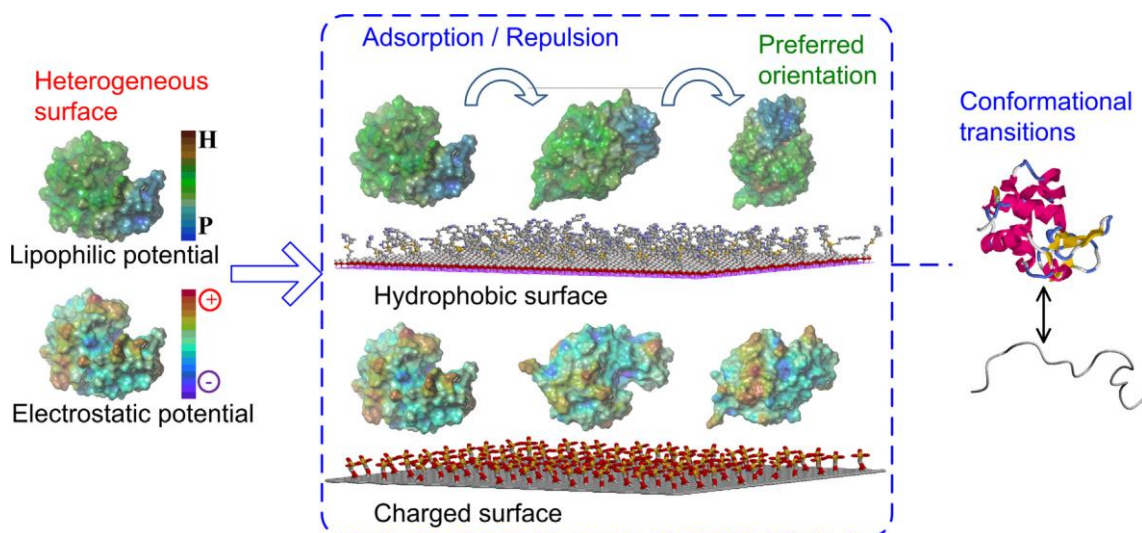





Figure 9 - Schematic diagram of chicken egg white lysozyme (CEWL) orientation at chromatographic surfaces at pH 7. CEWL heterogeneous surface is shown on the left panel and colored according to the lipophilic potential or the electrostatic potential. For lipophilic potential, brown is used for hydrophobic (H) and blue for hydrophilic (P). For electrostatic potential, red is used for positive (+) and purple for negative (-). Adapted from².

There are a number of factors that contribute to protein conformational transitions. BSA, for example, has several isomeric forms at different pH values³⁰ that are classified as: Extended (E); Fast migration (F); Normal dominant (N); Basic form (B), see Table 5. Solution pH leads to charge changes in protein residues, changing α -helix proportion and causing changes in different physical proprieties like aspect ratio, geometrical shape and total dimensions³⁰. All of these changed proprieties may alter the protein binding process.

Table 5 - Bovine serum albumin physical isomers physical parameters. Adapted from³⁰.

<i>Physical Parameters</i>	<i>BSA Isomers</i>			
	<i>E (Extended)</i>	<i>F (Fast migration)</i>	<i>N (Normal)</i>	<i>B (Basic)</i>
				
pH	2.7	4.5	8	10
% α -helix	36	45	55	48
Aspect ratio	11.9	3.2	2.6	
Geometrical dimensions	Oblate spheroid	Prolate	Triangle	
Size (nm)	2.1×2.1×25.0	4.0×4.0×12.9	8.0×8.0×3.0	

All things considered, protein adsorption onto any support can be a complicated process influenced by pH, temperature, ionic strength, protein conformational changes and the electrochemical and physical proprieties of both the protein and the solid phase³⁶.

1.6 Subprocesses of protein adsorption

A comprehensive understanding of the adsorption phenomena, and in particular its molecular mechanism, is crucial for the research and development of biomolecule chromatography. Many experimental techniques, for example, atomic force microscopy, nuclear magnetic resonance, X-ray crystallography, surface plasmon resonance, hydrogen-deuterium isotope exchange, confocal laser scanning microscopy, and titration calorimetry have been used to explore the microscopic information of the adsorption processes¹⁵. However, none of these techniques can detect the dynamics of the process, which restricts not only the adsorption mechanism understanding, but also the ligand design and process optimization¹⁵. Nevertheless, some light has been shed on the molecular mechanism of interaction. According to Yamamoto⁴² and Hearn¹⁸, the binding process of different biomolecules onto, respectively, ion exchange and hydrophobic interaction resins can be divided into at least five subprocesses^{18,42-46}:

1. Dehydration or/and removal of the protein electrical double layer (EDL);
2. Dehydration or/and removal of the solid phase electrical double layer (EDL);
3. The interaction between the protein and the solid phase;
4. The structural rearrangement of the protein upon adsorption;
5. Rearrangement of the excluded water or/and ion molecules in bulk solution.

Dehydration or removal of the protein electrical double layer (EDL). EDL theoretical concept will be further explained in this chapter. Prior to adsorption, water molecules or/and ions that surround the protein must be partially excluded. It was observed that hydrophobicity of a protein increases with size and exposed hydrophobicity surface area. Given that, proteins with larger exposed hydrophobic patches require more energy for this dehydration/de-counter-ion step. It is important to realize that this dehydration step is an energy consuming process in which enthalpy of adsorption increases. However, the entropy gain due to more release of water or ions usually results in higher degrees of freedom and compensates this unfavorable enthalpic increase¹⁸. This specific subprocess will be further addressed in this chapter from a thermodynamic point of view.

Dehydration or removing the EDL of the solid phase is necessary for protein adsorption. Water molecules and ions surrounding the ion exchanger are excluded⁴² in the same way of the first subprocess. It will depend on the properties of the solid phase, such as electrostatic state, functional groups and hydrophobicity.

The interaction between the protein and the solid phase. Both electrostatic interactions and/or nonspecific interactions such as hydrophobic interactions between the protein and ion exchanger mediated by van der Waals forces, and formation of bonds such as hydrogen

bonding or formation of coordination complexes can occur. These forces are usually accompanied by enthalpy release and entropy loss, giving this subprocess an important role in the determining the magnitude of the total adsorption enthalpy ^{18,42}.

The structural rearrangement of the protein upon adsorption. Fourier transform infrared spectroscopy with attenuated total reflectance (ATR-FTIR) procedures revealed that proteins undergo a large degree of structural rearrangement in liquid chromatography ⁴⁷. These structural changes are higher in bigger proteins that are considered “soft”, like BSA. Enthalpy change associated with this process obtained by microcalorimetry for BSA is between 4-10 mJ.m⁻², which shows that this is an endothermic process (due to being positive), at least in presence of hydrophobic solid phases ¹⁸.

Rearrangement of the excluded water or ion molecules in bulk solution contributes to the entropy increase. It is believed that this process is much more important in ion exchange adsorption mechanism ⁴² than in hydrophobic interaction adsorption ¹⁸.

This classification can be used to facilitate interpretation of the enthalpy changes measured by microcalorimetry or van't Hoff plot analysis to further elucidate the molecular adsorption mechanism from a thermodynamic point of view.

1.7 Thermodynamic aspects of interaction in chromatography

The possibility of a protein to be adsorbed (at constant pressure and temperature) is determined by the change in standard Gibbs free energy (ΔG°) of the system, which can be written for a reversible adsorption process:

$$\Delta G^\circ = (\Delta H^\circ - T\Delta S^\circ) < 0 \quad (1)$$

where ΔH° is the standard enthalpy change in the process and ΔS° is the standard entropy change. Exothermic events ($\Delta H^\circ < 0$) result in heat released by the system, while endothermic events ($\Delta H^\circ > 0$) leads to heat absorption.

Paying closer attention, for a process spontaneously occur, ΔG° must be negative. When the adsorption process results from an increase in enthalpy (positive values for ΔH°) the entropic effects are considered to dominate the adsorption process. In this case, the binding strength of the protein with the sorbent is generally expected to be enhanced by increases in temperature, as often occurs in the case of HIC¹⁸ and IEC^{48,49}.

Separation of different proteins is achieved by tuning its adsorption affinities for a specific solid phase. The equilibrium binding affinity constant (K) can be related to the standard Gibbs free energy (ΔG°) change for a specific protein-solid phase as:

$$\Delta G^\circ = -RT \ln K \quad (2)$$

where R is the gas constant ($8,314462 \text{ J.K}^{-1}.\text{mol}^{-1}$) and T is the absolute temperature in Kelvin. From equation 6 and 5 we can understand that for protein separation to occur, i.e. if proteins have different values for binding affinity (K), this can be associated with different ΔG° values which is related to different enthalpy and entropy values. Proteins can thus be separated by varying the magnitudes of the respective enthalpy or/and entropy changes, resulting in different binding affinities and different adsorption free energies changes.

1.7.1 Processes that can contribute to enthalpy and entropy change in IEC protein adsorption

It has been suggested and theoretically estimated^{42,50} that the major contributions to the entropy change, associated with protein adsorption, are the process of dehydration or/and the obliteration of the electrical double layer¹⁸. In both processes, changes in the structure of water play a major (and most likely the dominant) role because immediately prior to adsorption some of these water, solvent or electrolytes must be excluded to decrease the distance between the protein and the solid phase so that short-range interactions can occur.

According to past estimates from 1979 this dehydration step was exothermic ($\Delta H < 0$)⁵¹. We know now from direct measurements that this is the exception and not the rule. Surface and protein dehydration, in most cases, requires energy being actually an endothermic process ($\Delta H > 0$)^{18,29}. For example, solid phases with aromatic hydrocarbons have endothermic dehydration enthalpies but aliphatic hydrocarbons have negative dehydration enthalpies. Other studies showed that more hydrophobic proteins need more energy to dehydrate, and exhibit higher dehydration heats¹⁸. This observation indicated that both protein and solid phase dehydration is enthalpically unfavorable. The adsorption process occurs due to large entropy gains that compensates that enthalpically unfavorable condition. In other words, more hydrophobic proteins have more ordered water molecules around them, hence the need of larger energies to remove them. This does not mean that these proteins will have more difficulty in adsorbing because this energy is later compensated by the higher water molecule degrees of freedom gained, also known as, entropy gains. It was shown that interaction between globular proteins and HIC solid phases are dominantly governed by hydration/dehydration processes^{52,53}. It was found that the removal of water from protein polar groups carries a large enthalpic penalty⁵⁴ which explains the relatively large dehydration energy necessary.

According to Norde et al. structural rearrangements of proteins upon adsorption also contribute to entropy changes but not as significant as the hydration/dehydration processes. These rearrangements are believed to play more important roles in enthalpy changes. Also, positive ΔH values were obtained for this subprocess, using flow microcalorimetry when BSA is adsorbed onto negative charged surfaces^{18,37,55,56}.

There are other interactions that may have an influence on the enthalpy changes. For instance, the attractive electrostatic forces between the protein and the charged resin are expected to generate a larger heat release when compared to the hydrophobic interactions¹⁸. According to Ross et al., ionic interactions have negative ΔH or sometimes, slightly positive ΔH ³⁹. Generally, electrostatic interactions play an important role in determining the magnitude of the adsorption total enthalpy. However, this does not mean that protein adsorption in IEC is solely driven by enthalpy changes, as observed by prior studies^{18,29,57}.

More examples of other interactions are the double-layer, Born and hydration repulsion effects that occur when the diffuse layers start to approach each other. Born and hydration repulsion forces resulting from the overlapping of electron orbitals difficult the removal of water molecules from the interfacial region and prevent strong attractive interactions between the protein and the solid phase. These repulsive forces contribute mostly to the increase of positive enthalpy change, leading to unfavorable conditions for protein binding¹⁸. At the same time, as it will be more precisely mentioned in sub-chapter 1.8, these forces are of utmost importance to avoid irreversible bounding between the solid phase and protein.

In summary, Table 6 and Table 7 are presented to assemble all the processes that are currently believed to be responsible for thermodynamic changes in a chromatographic system.

Table 6 - Summary of events responsible for thermodynamic changes in a chromatographic system. Note that some of these events are interconnected and all are highly related.

<i>Enthalpic events</i>	<i>Entropic events</i>
EDL overlapping ¹⁸	Dehydration and hydration ¹⁸
Ionic interactions and van der Waals ^{37,39}	Abolition of EDL ¹⁸
Dehydration ²⁹	Structural rearrangements upon adsorption (although with a low significance) ^{18,50}
Electrostatic interactions ²⁹	
Born and hydration repulsion forces ¹⁸	
Hydrogen bonding ³⁹	
Structural rearrangements upon adsorption ^{18,37,50}	
Interaction between adsorbed proteins ³⁷	

Table 7 - Expected signs of the enthalpic processes based in upon a large body of thermodynamic results for protein-ligand association in solution and protein-solid phase interaction. Adapted from Ross et al. ³⁹

<i>Process</i>	<i>ΔH</i>
Dehydration (partial withdrawal of the water from protein nonpolar groups) ^{18,39}	Positive
Van der Waals ^{36,39}	Negative
Hydrogen bonding (in low salt medium) ³⁹	Negative
Ionic or electrostatic interaction ^{31,39}	Negative or slightly positive
Protein protonation ³⁹	Negative
Protein conformational changes ^{37,56}	Positive
Reorientation and rotation in IEC solid phase ²⁹	Positive
Repulsive forces between same charges or between hydrophilic moieties and hydrophobic groups ^{29,37}	Positive

Historically, two methods have been employed to obtain information about thermodynamic quantities associated with liquid chromatographic adsorption: van't Hoff plots analysis and microcalorimetric measurements. Despite microcalorimetry enthalpy measurements being more reliable, they require more demanding experimental operation procedures and skillful interpretation and are time and reagent consuming ¹⁸.

1.7.2 Van't Hoff plot analysis

Van't Hoff analysis is an indirect method to measure thermodynamic quantities associated with liquid chromatography in which the enthalpy and entropy changes can be obtained by joining equations 1 and 2 obtaining the following van't Hoff linear expression:

$$\ln(K) = \frac{-\Delta H^{\circ}}{R} \left(\frac{1}{T}\right) + \frac{\Delta S^{\circ}}{R} \quad (3)$$

ΔH° and ΔS° may not change linearly with temperature in the case of proteins, making, as always, the analysis of biomolecules systems more complex. Plotting the natural logarithm of the retention data, against the inverse of the absolute temperature in Kelvin, as shown on Figure 10, allows us to calculate the enthalpy and entropy of a given system. Just by observing the slope we can see if the process is mainly exothermic or endothermic. Also, the indirect method of van't Hoff analysis is disabled by the presence of multiple subprocesses associated with adsorption and thus does not produce representative results of the complex protein adsorption mechanism, especially in overloaded conditions^{18,29}.

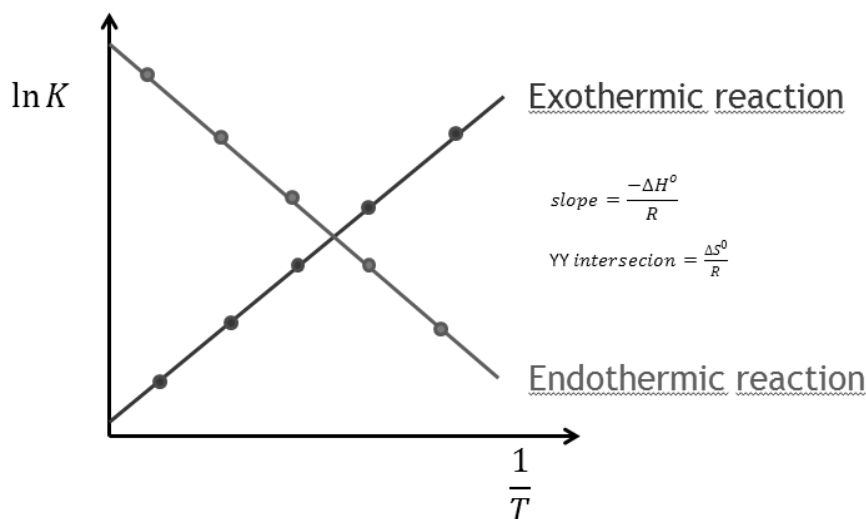


Figure 10 - Examples of two van't Hoff plots for two types of reactions. This linear behavior is rarely observed when studying biomolecules.

1.7.3 Microcalorimetry techniques

Microcalorimetric techniques have the ability to investigate and enlighten complex adsorption mechanisms in liquid chromatography based on acquired thermodynamic parameters^{29,31,37,42,58-61}.

There are some discrepancies when thermodynamic values obtained from van't Hoff analysis when compared to microcalorimetric data. On the other hand, enthalpy changes from microcalorimetric data are directly measured opposed to standard-state values from van't Hoff analysis. Therefore, direct measurement of protein processes by microcalorimetry is

more beneficial since these will reflect more heterogeneous circumstances that will prevail in biological systems^{18,48}. Two techniques may be used to carry out microcalorimetric studies: isothermal titration calorimetry (ITC) and flow microcalorimetry (FMC).

1.7.3.1 Isothermal titration calorimetry

A decade ago, the isothermal titration calorimeter (ITC) was considered as a specialist apparatus; few laboratories had access to one and even fewer understood the implications of much of the data generated. Currently, ITC instruments can be found in hundreds of laboratories, whose specialities in biological areas range from determining affinities for whole cellular systems to drug design. This rapid flourishing of the method and widespread availability of data has dramatically increased our understanding of many systems. It has also provided crucial data towards improving our ability to predict thermodynamic parameters for biomolecular processes⁶².

ITC directly measures the enthalpy change for a bimolecular binding interaction at a constant temperature. This methodology relies upon a differential cell system within the calorimeter assembly. The reference cell contains only water or buffer, while the sample cell contains the macromolecule or ligand as well as a stirring device. Injection of the second component into the sample cell produces heat effects that are due to stirring, dilution of the ligand, dilution of the macromolecule and the heat of the interaction.

Some examples of biological studies where ITC can be used are: protein-protein and protein-peptide interactions involved in such diverse processes as cell signalling; alzheimer's disease; transcription; chaperones and muscle contraction. In recent years, studies have described the utility of the technique in the study of protein-drug, drug-DNA, protein-DNA and protein-carbohydrate interactions⁶² and as expected, biomolecule-solid phase interactions in chromatography^{18,35,42,43,43-46,58,63}.

Nevertheless, ITC based studies present some limitations in understanding adsorption mechanism in chromatography. An ITC cell does not quite replicate the dynamics of a chromatographic process nor permits the observation of several substeps during time in the adsorption process. These disadvantages are overcome by the more recent use of flow microcalorimetry (FMC). When protein adsorption involves multiple phenomena, like the ones previously mentioned, exothermic and endothermic changes have been observed at different times during the adsorption process, as indicated by the FMC technique^{29,31,37}.

1.7.3.2 Flow microcalorimetry

Flow microcalorimetry (FMC) has the same objective than ITC, namely the measurement of enthalpy changes during interaction between two molecules at a constant temperature. Also, it is an effective approach to real-time heat signal measurements, since evaluates both adsorption and desorption events occurring in a chromatographic column, thus allowing a

better understanding of the forces that drive the adsorption process^{29,31,37,48,52,58,59,64,65}. Also, as the reader may see in Figure 11, FMC shares with a chromatographic system the same mode of operation, therefore the results are expected to represent what *really* happens in a chromatographic column. Highly sensitive thermistor sensors, placed in the column volume, are responsible for measuring very small power changes (10^{-7} W). These energy changes are converted to heats of adsorption using an experimentally determined calibration factor³⁷.

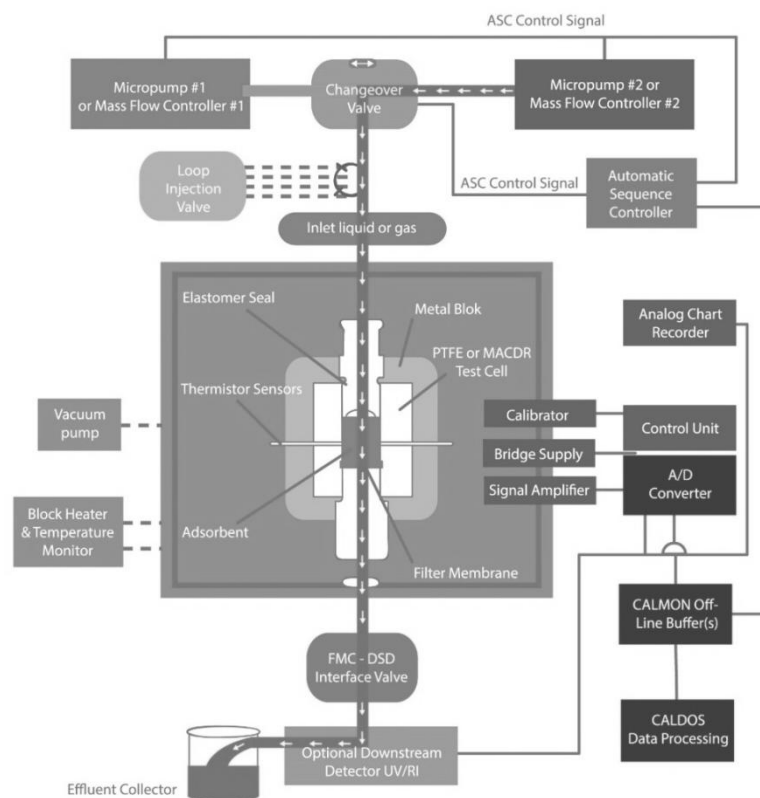


Figure 11 - Schematics of a flow microcalorimetry system and all its constituents.

These characteristics make FMC the only experimental technique to date, that can be used to in-situ study of molecular adsorption interactions during chromatography. And without interfering with the thermodynamic and kinetic adsorption equilibrium. This technique has been used in different types of chromatography, i. e. hydrophobic interaction chromatography⁵⁹, ion exchange chromatography^{29,36,48}, affinity chromatography⁶⁶ and with several types of biomolecules such as proteins^{29,36,37,48,66} and more recently with pDNA³¹.

A typical output from FMC is a graph like the one in Figure 12, which may be called a thermogram. In essence is a plot of heat in $\mu\text{J}\cdot\text{s}^{-1}$ versus time in seconds. The thermogram may be shaped by only negative heats, only positive heats or both. Note that the negative peaks here represent endothermic events and positive peaks exothermic ones due to the reference system used. In other words, if the thermistors sense a heat decrease, a negative peak will

appear, but that energy was transferred/absorbed by the protein-solid phase system, consequently it will be an endothermic event, because the studied system gained energy.

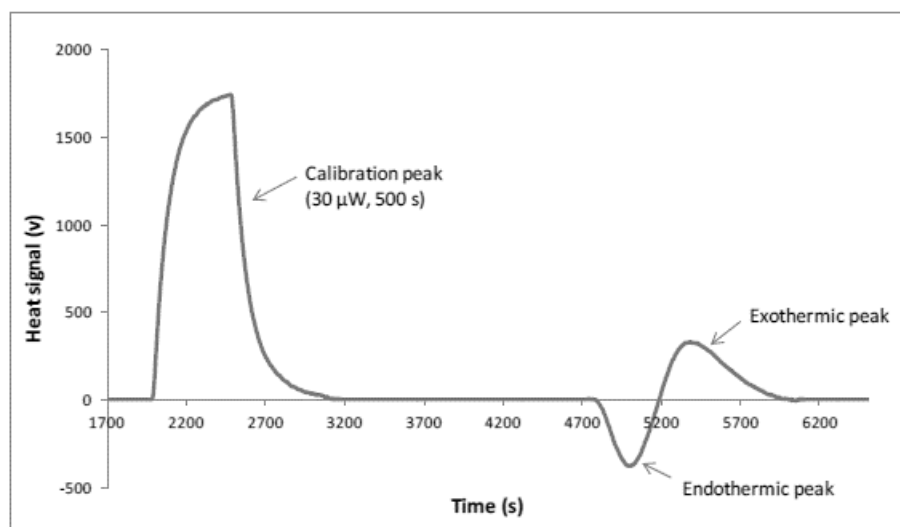


Figure 12 - Example of a characteristic thermogram showing an electrical pulse given to the system (calibration peak) followed by an endothermic and exothermic events. Represented with consent of the author⁶⁷.

Flow microcalorimetric methods allow the measurement of the heat flow during the chromatographic process for any range of product concentration. Through the knowledge of the magnitude and chronology of thermal events during and after the biomolecule-adsorbent interaction, the adsorption mechanism can be elucidated.

1.8 Theoretical aspects of adsorption mechanism in preparative chromatography

Maturity of preparative chromatography will be only reached when it is possible to model and predict its operation for any range of product concentrations. During the last years researchers have presented several empirical, semi-empirical and theoretical equilibrium models to describe and elucidate molecule adsorption mechanisms⁶⁸. Some of the used approaches are presented below.

Adsorption equilibria is usually described by the relation between free protein concentration (C) and the adsorbed protein concentration (Q) in the solid phase. In liquid-solid systems this relation is temperature dependent, hence usually determined at a constant temperature, so it is called adsorption isotherm. Adsorption isotherms data is very valuable for process analysis, design and optimization of adsorption chromatography.

1.8.1 Langmuir model

Among several models, the Langmuir one (equation 1) is the most widely used to explain adsorptive phenomena in chromatography⁶⁸:

$$Q = \frac{Q_m K_a C}{1 + K_a C} \quad (4)$$

where Q_m is the maximum adsorption capacity and K_a is the association constant of a molecule to the adsorbent. Maximum adsorption capacity is widely used to compare different solid phases and molecules. At low protein concentration, if one has $K_a C \ll 1$, equation 1 can be reduced to linear isotherm expression (Henry isotherm):

$$Q = mC \quad (5)$$

where m is a constant. Figure 13 shows a graphical representation of an adsorption isotherm that follows Langmuir model.

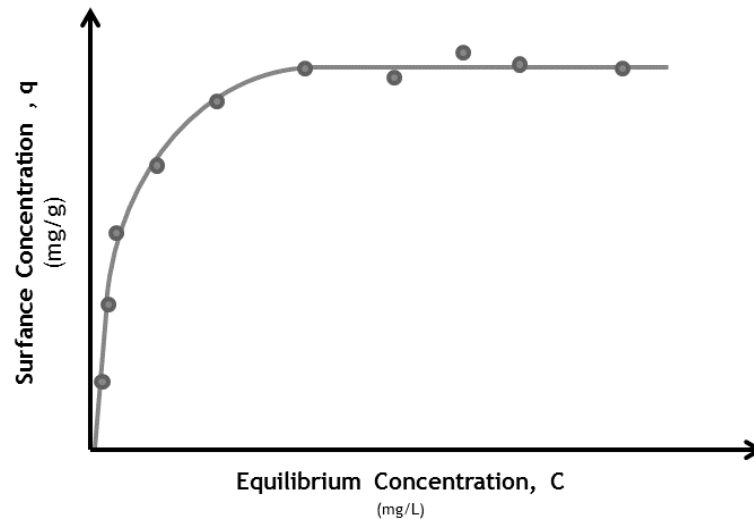


Figure 13 - Adsorption equilibrium isotherm example. Obtained plotting surface concentration of a given molecule versus the concentration obtained after the equilibrium.

The Langmuir theory from 1918, originally developed for gas adsorption, is advantageous because of its simplicity and wide applicability. It is based on three essential assumptions that do not quite hold for the adsorption of biomolecules like proteins: monolayer coverage, binding sites equivalence, and binding sites independence. Langmuir himself stated the limits of his now famous equation commenting: *“Considering the nature of the simplifying assumptions made in its derivation it should, of course, not be looked upon as a general equation of the adsorption isotherm”*⁴⁰. Nowadays, Langmuir equation is regarded as an empirical expression when applied to liquid-solid adsorption systems. In other words, Langmuir-type behaviors are experimentally observed.

1.8.2 Steric mass action model

Typically, proteins have polyelectrolyte characteristics and their adsorption behaviors are more complex, as explained before. Protein adsorption depends more on the features of small regions of the protein surface rather than the surface as a whole, as previously explained. These contact regions in liquid phase will associate with solvent or counter-ions by solvation and electrostatic interaction. In ion exchange adsorption these solvent molecules or ions bound to the protein are displaced, which is assumed to obey a stoichiometric relationship. The steric mass action model (SMA) has been recognized for taking this ion displacement into account and focus the salt concentration effect on the adsorption⁶⁹. SMA model also accounts for the steric shielding effect of binding sites by the bound protein, as described below:

$$C = \left(\frac{Q}{K_a} \right) \left(\frac{C_s}{A - (z + \sigma)Q} \right)^z \quad (6)$$

where C_s is the salt concentration, z is the characteristic charge of protein, A is the ionic capacity of the ion exchanger, and σ is the steric factor of the protein. The SMA model

expresses the effect of ionic strength on the adsorption equilibria of a protein to an ion exchange adsorbent.

Although these models offer a strictly theoretical framework to understand adsorption, it is usually difficult for a biomolecule obey all the strict assumptions made in the model development due to biomolecule complexity and adapting capacity. This limits the applicability of the models in protein chromatography¹⁵. Nonetheless, there are also semi-empirical thermodynamic models⁷⁰ to describe polypeptide and protein binding to chemically modified surfaces.

1.8.3 Potential barrier chromatography theory and electrical double layer

In order to adequately discuss adsorption from the viewpoint of the interaction thermodynamics, a useful starting point is the concept of potential barrier chromatography (PBC).

Potential barrier chromatography emphasizes the relationship between energy trajectory for the binding of protein(s) or polypeptide(s) and the overall distances of their approach to the solid surface. The interaction potential in PBC is a result of added effects like van der Waals attraction, Born and hydration repulsion and electrical double layer effects.

The electrical double layer (EDL) is a phenomenon on the surface of any charged object when it is exposed to a fluid with free ions, like in protein solutions. There are two parallel layers of charged ions surrounding the solid phase and the protein (either positive or negative), see Figure 14. The first layer, or Stern layer, comprises ions adsorbed onto the solid phase or the protein. The second layer is composed of ions attracted to the surface charge via Coulomb force, electrically screened by the first layer. This second layer is loosely associated with the solid phase or protein, being made of free ions that move in the fluid under the influence of electric attraction and thermal motion rather than being firmly anchored. It is thus called the "diffuse layer". When two different diffuse layers begin to overlap, namely if the protein has opposite charge of the solid phase, alterations in the distribution of ions result in a negative free energy change of the system which is a favorable thermodynamic event.

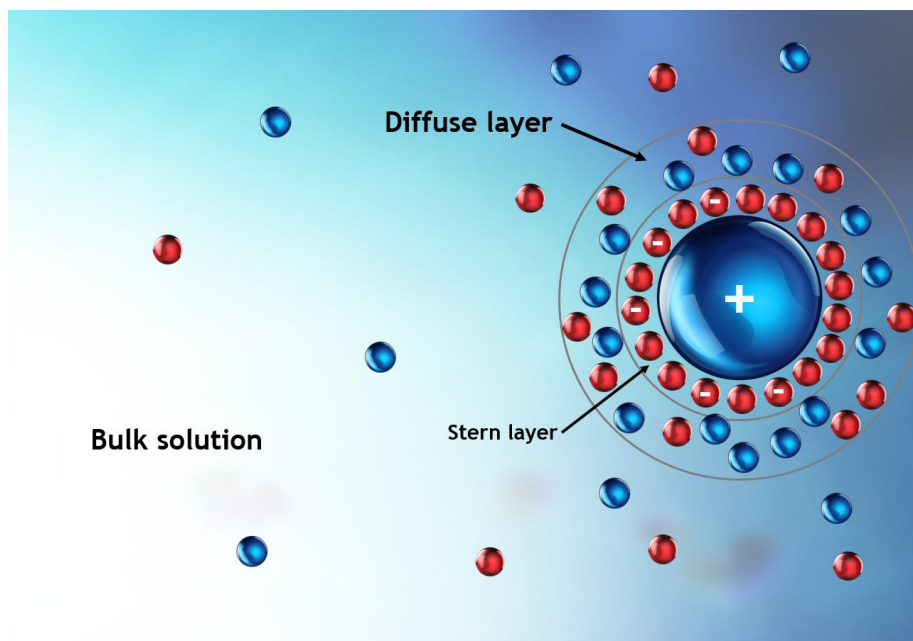


Figure 14 - Electrical double layer scheme of a positively charged molecule. Negative ions are represented in red and positive charged ions are represented as blue.

In contrast to double layer effect long-range process, the Born effect is a short-range phenomenon that occurs due to electron orbital overlapping. Hydration repulsion effect arises from the difficulty in removing water molecules from the Stern layer of ions ¹⁸. The total interaction potential (\emptyset) therefore can be described as:

$$\emptyset = \emptyset_{DL} + \emptyset_B + \emptyset_{vdw} \quad (7)$$

where \emptyset_{DL} is the potential of the electrical double layer interaction, \emptyset_B is the potential of the Born repulsive effect and \emptyset_{vdw} is the potential of the van der Waals forces. Since these forces are a function of the approach distance (d_h) between the protein and the solid phase, the energy net potential (\emptyset) can be plotted against this distance, as shown in Figure 15.

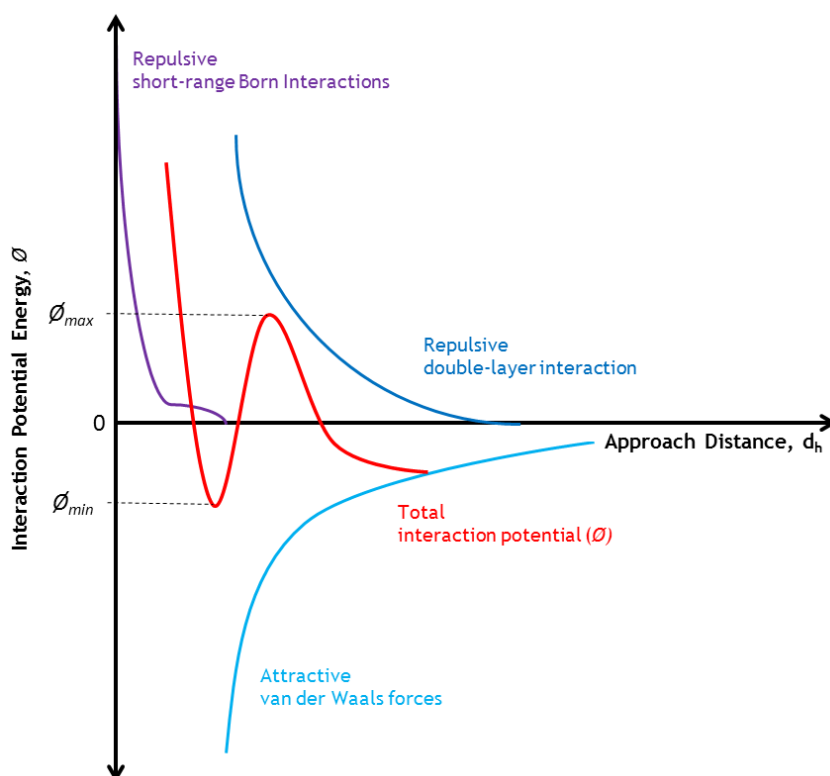


Figure 15 - Interaction Potential energy profiles relevant to potential barrier chromatography. Red line represents the total interaction potential with the location of the maximum, ϕ_{max} , and minimum, ϕ_{min} , of the interaction potential energy profiles associated with the adsorption energy well and the potential barrier respectively. Adapted from ¹⁸.

These interaction potentials can be influenced by numerous experimental factors, for example, the ionic strength or pH of the mobile phase. The profile shown in red is the total interaction potential constituted by the sum of all the individual interactions potential energies established by the protein and the solid phase. Strong van der Waals attractions tend to generate deep adsorption energy well(s), while double layer repulsion effects and short range repulsion interactions prevent the occurrence of such deep wells. The potential energy well (ϕ_{min}) should not be too negative because it must be compatible with elution, as previously explained. While in contrast, no adsorption is feasible until an energy barrier (ϕ_{max}) is properly overcome ¹⁸.

Various fundamental questions can be asked about the magnitude of all these processes and forces, namely how do the individual subprocesses can influence the interaction mechanism between the protein and solid phase and how can the interaction thermodynamics be elucidated? The importance of understanding in detail all of these individual subprocesses have already been reported by other authors ^{18,42}.

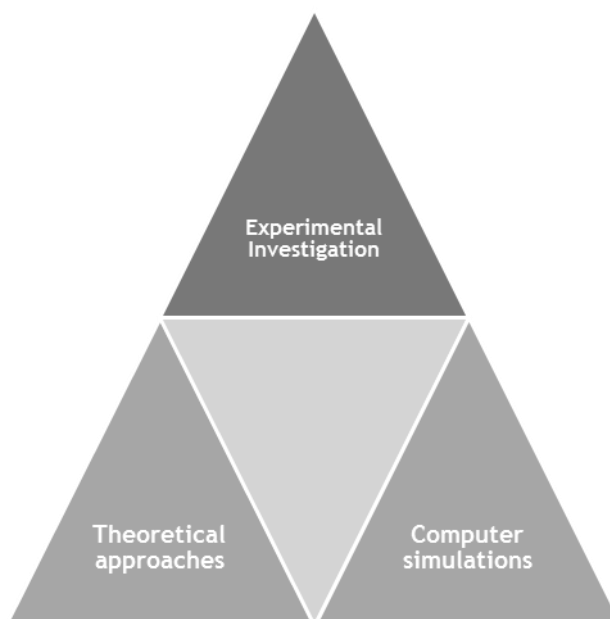
Computer simulated models using Monte Carlo or molecular dynamics simulations ^{20,24,34} have been, more recently, also used to study chromatographic processes. Nonetheless, for any

discussion to be consistent and have a physically relevant meaning, the mechanisms underlying chromatography of biomolecules need to be experimentally understood².

Chapter 2 - Goal of the study

As previously mentioned, the importance of protein molecules in recent technologies is well recognized. Regarding the whole recombinant protein production, the most challenging step is usually its purification. Preparative anion-exchange chromatography techniques have been widely used in protein purification due to the highest binding capacities presented¹³. Hence, a higher understanding and further elucidation of the complex interactions that contribute to protein adsorption phenomena is required.

Taking all this information into account, the main goal of this work is to study the mechanism of protein adsorption, namely BSA, onto several commercially available solid phases with charged ligands using the FMC technique and batch adsorption to experimentally obtain adsorption isotherms curves and support's static binding capacity¹³. By combining these data with state of art information, like computer molecular simulations, theoretical approaches and other experimental investigations, the final objective is to further elucidate the mechanism from a thermodynamic point of view so that there could be an improvement in the knowledge of protein behavior at charged surfaces, which ultimately leads to the possibility of future development of newer and superior chromatographic solid phases.



Results for TSKgel SuperQ 5PW and TSKgel SP 5PW from TOSOH BIOSCIENCE were compared with previous studied supports that differ in their ligand attachment technologies, namely Toyopearl DEAE⁷¹ and Toyopearl GigaCap⁷². TSKgel SP although being a cation exchanger, was used in order to evaluate the thermodynamic differences in non-binding conditions with an effort to understand the weaker forces of the inherited mechanism.

Chapter 3 - Materials and Methods

3.1 Adsorption isotherm measurements

Several BSA (Sigma-Aldrich, USA) solutions were prepared in 20 mM Tris-HCl buffer (Nzytech, Portugal) at pH 9. One solution contained 50 mM of NaCl (Fisher Chemical, UK) and the second was void of any salt. The solid phases TSKgel SP 5PW and TSKgel SuperQ 5PW kindly offered by TOSOH Bioscience (Germany) were washed with distilled water and later with the respective buffer solution to guarantee the same volume due to swelling. 1mL of known concentration BSA solutions, , were then transferred to 12-well plates and 10 μ L of solid phases suspension (1:2) was placed in each well. The plates were sealed with parafilm and agitated for 16 h at 230 rpm in a 21.5°C orbital shaker. Initial BSA solutions were kept at room temperature, preliminary experiments showed that there was no significant difference between leaving BSA initial solutions at 21.5°C or room temperature. Also, prior experiments showed that BSA molecules did not adsorb into 12-well plate walls, and 12-well plates did not release any molecule that interfere with BSA concentration determination (data not shown).

After equilibrium, the slurry was transferred to eppendorf tubes and left to sedimentate by gravity for 20 minutes. The supernatant was separated from the adsorbent with a 0.22 μ m pore low protein binding syringe filter (Millex-GV, Merck KGaA, Germany). The absorbance of each solution, prior and after the equilibrium was then aliquoted to 96-well UV transparent plates (Thermo Scientific, Portugal) and BSA concentrations were determined at 280 nm with a UV spectrophotometer (Bio-rad, Portugal). A mass balance was performed in order to know the exact amount of protein bound to the adsorbent, and BSA equilibrium concentration were plotted against surface concentration. All salts used were of analytical grade. De-ionized distilled water obtained with Milli-Q ADV (Millipore, Madrid, Spain) was used in the prepared solutions.

3.2 Flow microcalorimetry

BSA adsorption thermograms were obtained using a flow microcalorimeter (Microscal FMC 4 Vi, Microscal Limited, UK) shown in Figure 16. It is operated in a similar way to a liquid chromatograph. The 171 μL cell (or column) is located between two highly sensitive thermistors that can detect power changes in the order of 10^{-7} W³⁷. Calibration was done providing the FMC with 3 μW during 100 seconds with the resin inside the cell, which corresponded to 0.3 mJ. Solutions flow through the cell using precision syringe pumps (Harvard Apparatus, UK) at 1.5 mL/h. Experiments were performed as Silva et al.²⁹ described. The system was packed with 171 μL previously washed solid phase suspended in approximately 500 μL of equilibrium buffer. Thermal equilibrium was reached by flowing the equilibration buffer 20 mM Tris-HCl pH 9 with and without 50 mM NaCl for approximately 12 h. After that, a configurable 30 or 230 μL loop was filled with BSA dissolved in the equilibration buffer and then injected into the column. Flow through was collected in falcon tubes and a mass balance was done to evaluate the adsorbed quantity. Between each injection, 20 mM Tris-HCl pH 9 with 1 M NaCl was used as elution solution and 0.5 M NaOH (José Manuel Gomes dos Santos Lda., Portugal) was used as a cleaning-in-place solution.

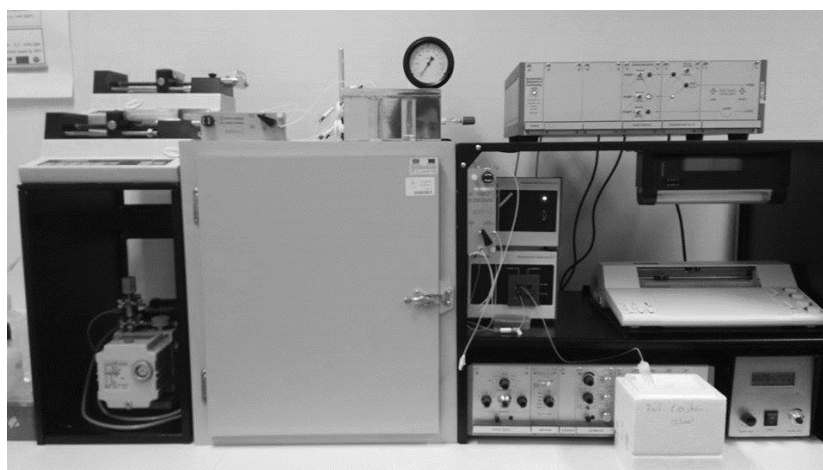


Figure 16 - Flow microcalorimeter used in the experiments of this work at CICS-UBI.

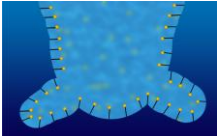
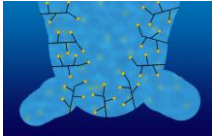
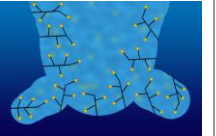
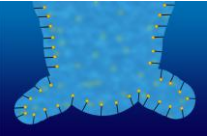
Acquisition, storing and data processing was made by CALDOS 4 software (Microscal, Limited, UK). Peak deconvolution and peak area calculation was performed with PeakFit 4.12 software (Seasolve Software Inc., USA) using asymmetric Gaussian peaks and Residuals method with a Savitsky-Golay type smoothing. The heat of adsorption of each step was calculated from the area of the de-convoluted peaks, to facilitate the elucidation of enthalpic events in the obtained thermograms.

Chapter 4 - Results and Discussion

4.1 Resins structural differences

Structural differences between the studied solid phases according to the supplier are shown in Table 8. Static binding capacity and affinity constant present in the table were obtained based on isotherm data by a linear regression of the Langmuir linearized equation. As stated by the provider, a traditional ligand attachment method (TSKgel SP and Toyopearl DEAE) consists of attaching the ligand directly to the resin through a spacer arm. The second generation attachment (TSKgel SuperQ) adds a carbon spacer network between the bead surface and the ligand. Ligands are also attached along the length of the spacer network, improving capacity. The third generation (Toyopearl GigaCap Q) ligand is just like the second but moves the charged groups to the larger pores where protein has better access to them, with the aim of increasing mass transfer speed and promoting faster desorption. The absence of ligands in smaller pores is not necessarily a disadvantage for protein separation, because induces a reduced elution volume⁷³.

Table 8 - Structural parameters of the studied resins together with the observed static binding capacity and affinity constants calculated from Langmuir linearized equation.

Features	Toyopearl DEAE - 650M	Toyopearl GigaCap Q - 650M	TSKgel SuperQ 5PW	TSKgel SP 5PW
Ligand	Anion exchanger -O-CH ₂ -CH ₂ -HN ⁺ -(C ₂ H ₅) ₂	Strong Anion exchanger -O-R-N ⁺ -(CH ₃) ₃		Strong cation exchanger -O-R-O-CH ₂ -CH ₂ -CH ₂ -SO ₃ ⁻
Mean pore diameter	100 nm			
Ion Exchange Capacity (meq/mL)	0.11	0.14		0.09
Bead Backbone	Hydroxylated polymethacrylic polymer beads.		Same methacrylic polymer chemistry but with a higher degree of crosslinking, making a more rigid bead.	
Attachment type	Traditional 	Third Generation 	Second Generation 	Traditional 
Static Binding Capacity (BSA)	42.7 ± 6.0 mg.mL ⁻¹	151 ± 18 mg.mL ⁻¹	109.3 ± 3.7 mg.mL ⁻¹	13.8 ± 2.4 mg.mL ⁻¹
Dynamic binding capacity (BSA)⁷³	25 g / L-gel	173 g / L-gel	52-88 g / L-gel	n.a.
Affinity constant (Ka)	10.8 ± 6.1 mL.mg ⁻¹	83 ± 34 mL.mg ⁻¹	15.6 ± 2.3 mL.mg ⁻¹	8.5 ± 4.4 mL.mg ⁻¹

It is important to refer that TSKgel SP, although being a cation exchanger sharing the same net charge with the protein, adsorption occurs. Even though an adsorption isotherm in these conditions was not found in literature, this “non-binding conditions” phenomenon has already been observed several times³⁷, and it is currently explained by the protein heterogeneous surface⁴⁰. Negatively charged proteins adsorbing onto negatively charged surfaces tend to expose positively charged regions independently of their net charge^{28,40}. As expected, TSKgel SP curve showed the lowest static binding capacity (Table 8 and Figure 17).

4.2 Adsorption isotherms data

The experimentally obtained adsorption isotherms for BSA are reported in Figure 17. By analyzing the profiles, it can be observed that all the supports follow a linear trend at lower concentrations, followed by a plateau. A type I Langmuir isotherm profile can be observed at lower protein equilibrium concentrations in all studied cases^{68,74}. This plateau is followed by a region of increasing capacity in the case of TSKgel SP and Toyopearl DEAE. One possible explanation for this second increase is the formation of multiple layers of BSA at the surface, or even protein structural rearrangements that makes it possible to accommodate more molecules, as already observed⁵².

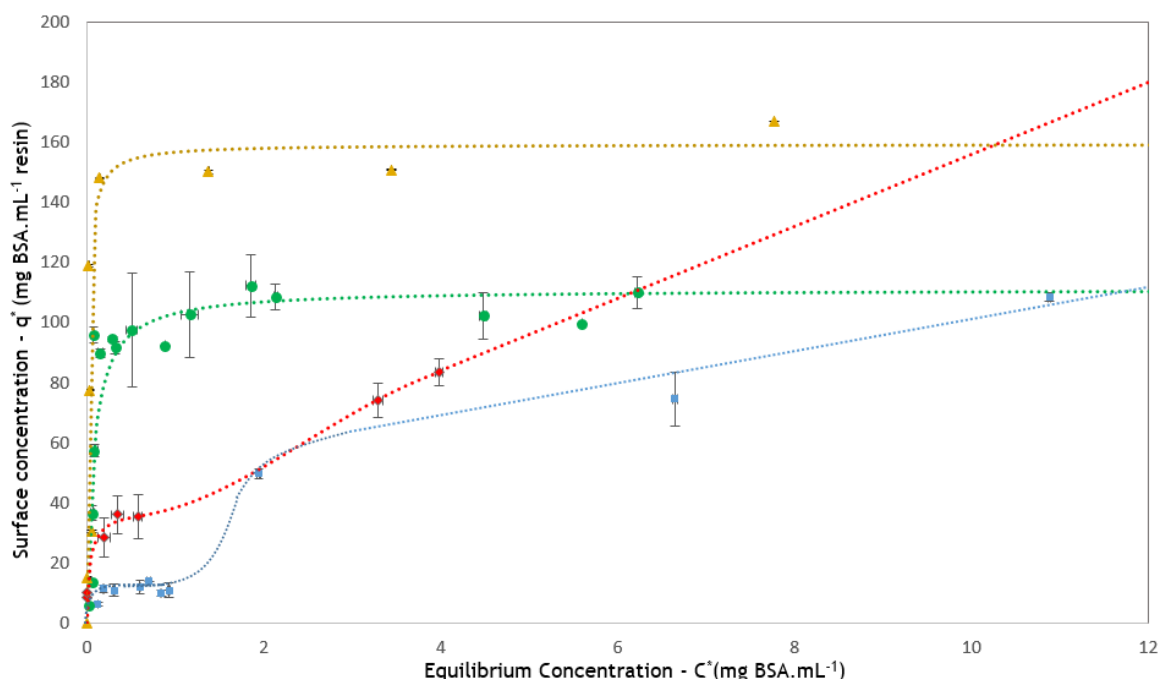


Figure 17 - Equilibrium binding isotherms for bovine serum albumin adsorption onto ion exchange resins at Tris-HCl pH 9 and 295 K. (●) TSKgel SuperQ 5PW, (◆) Toyopearl DEAE 650M, (▲) Toyopearl GigaCap Q-650M (■) TSKgel SP 5PW.

It can be seen that second and third generation solid phases have, as expected and according to supplier's information, higher static binding capacities. This is also justified by the type of ligand and ion exchange capacity since TSKgel SuperQ and Toyopearl GigaCap share the same type-Q cationic ligand unlike Toyopearl DEAE (bearing a DEAE-type ligand). Also, type-Q ligand has a relatively higher charge than DEAE-ligand at pH 9 ⁷⁵.

Still, Toyopearl DEAE binding capacity is largely superior than TSKgel SP binding capacity, which is expected since at these conditions TSKgel SP shares the same net negative charge with the used protein. Although being a cation exchanger, it was used expecting a weaker primary interaction between BSA and the solid phase in order to evaluate the thermodynamic differences and try to understand weaker forces of the inherited mechanism. This has already been successfully performed with BSA by previous authors ³⁷.

4.3 Microcalorimetric data

Following the adsorption isotherms measurements, microcalorimetry studies were performed in order to better understand the differences in the adsorption mechanism. Figure 18 shows the resulting thermograms of different microcalorimetric experiments. Different thermograms were obtained with similar injection protein concentrations (50 mg.mL^{-1}) and similar surface concentrations ($24.15 \pm 2 \text{ mg.mL}^{-1}$ gel). The profile of the thermogram curve is analogous for the anion exchangers Toyopearl DEAE, Toyopearl Gigacap and TSKgel SuperQ. In the first moments of the adsorption the mechanism is majorly endothermic while in the latter part of the process the microcalorimeter detects slight heat rises, indicating exothermic event(s). Although this behavior is the same for all the positively charged supports in these conditions, the intensity, timing, area, and shape of the peaks varies greatly.

It is important to keep in mind that although endothermic energies are positive, they are shown as negative in thermograms. Thermograms are presented in the calorimeter perspective, i.e. a heat loss (negative heat) for the microcalorimetry is actually a heat gain from the resin-protein system.

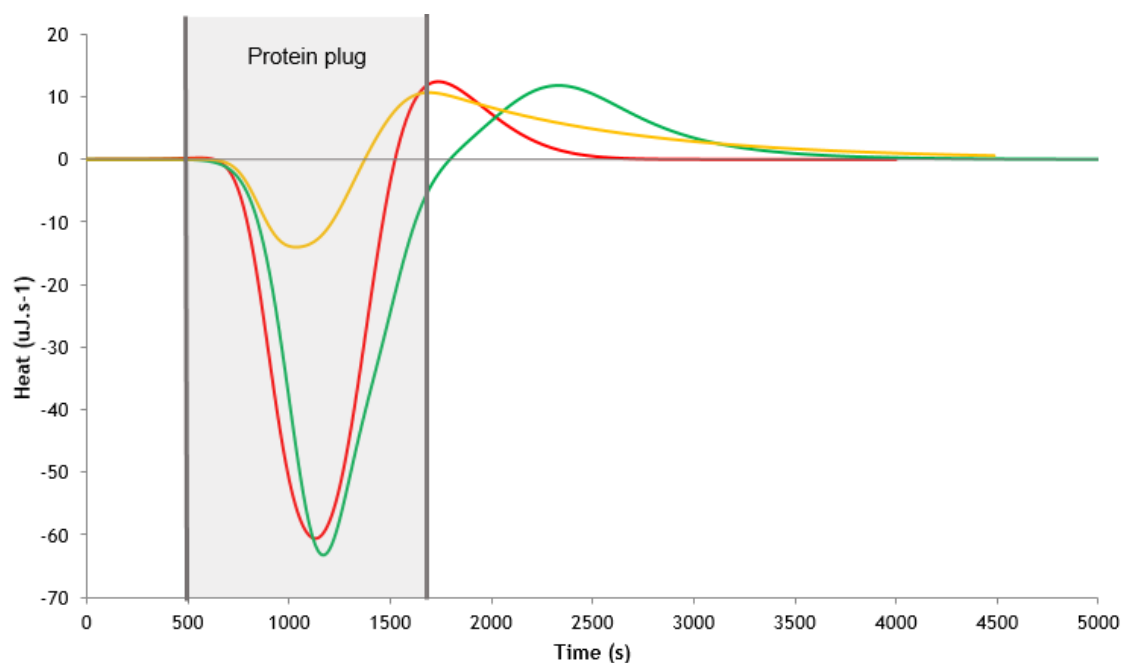


Figure 18 - FMC thermogram obtained for $230 \mu\text{L}$ injection of 50 mg.mL^{-1} BSA in equilibrium buffer Tris-HCl pH 9 adsorbing onto (●) TSKgel SuperQ 5PW, (◆) Toyopearl DEAE 650M and (▲) Toyopearl GigaCap Q-650M. Surface concentration (and flowthrough %) are respectively, 21.5 mg.mL^{-1} resin (66 %), 27.66 mg.mL^{-1} resin (52%) and 23.28 mg.mL^{-1} resin (61%). Shaded area represents the interval of time at which the protein plug contacts with the support.

Peak deconvolution using PeakFit Software was performed in order to separate more clearly the different events as already done before by previous authors ^{29,31,37}. An example of a possible peak deconvolution is shown on Figure 19. Paying closer attention, not only there is

an overlapping between exothermic and endothermic events, but the endothermic peak has a subtle “shoulder”, particularly more notorious in low surface concentrations as the reader may observe in Figure 19 and in Appendix I. Possibly the “shoulder” in the endothermic part is more visible at lower concentrations due to not being masked by the exothermic one. Therefore, this suggests the possible overlapping of different events during the adsorption process. We can see the appearance of an extra endothermic peak, which evidences the complexity of the adsorption mechanism.

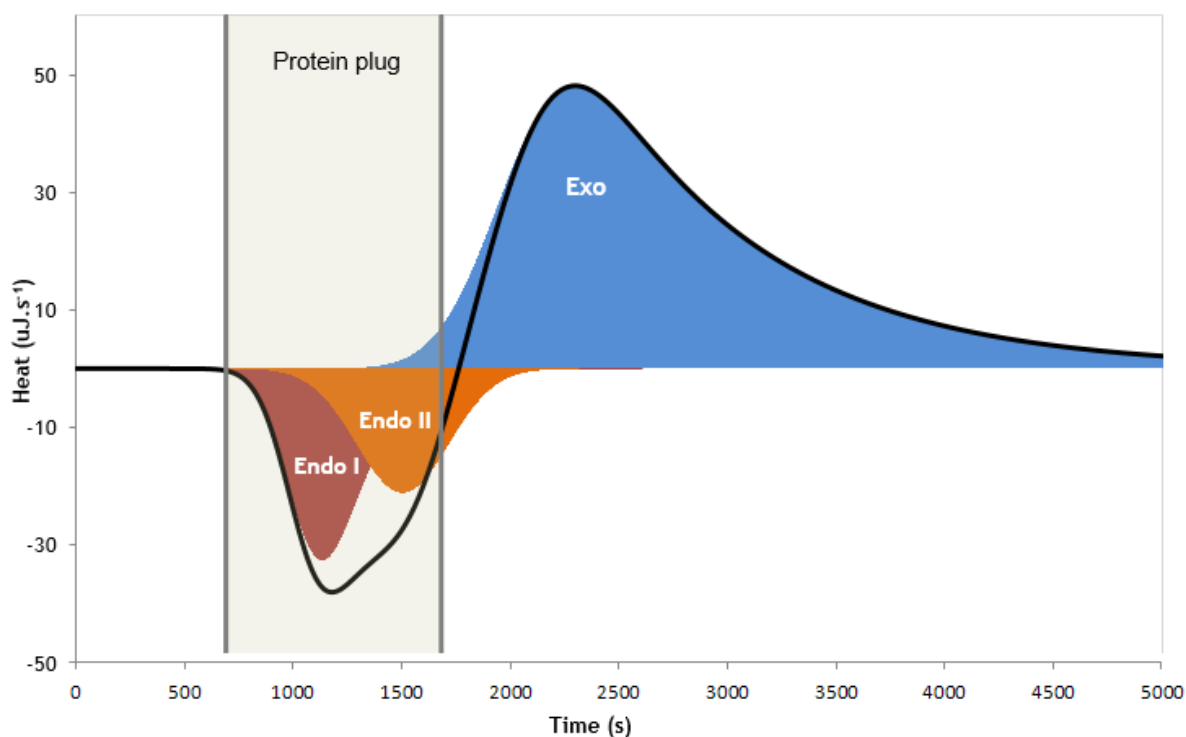


Figure 19 - PEAKFIT deconvolution of thermogram for BSA adsorption onto TSKgel SuperQ 5PW with Tris-HCl pH 9 for 230 μL injection of 50 $\text{mg} \cdot \text{mL}^{-1}$ resulting in surface concentration of 8.37 $\text{mg} \cdot \text{mL}^{-1}$ resin. Shaded area represents the interval of time at which protein flowed through the cell.

Considering the mechanism proposed by Yamamoto and co-workers⁴² mentioned in the first chapter. The adsorption process at a molecular level can be divided in several sub-processes:

- (1) water molecules and ion release from the protein and support;
- (2) interaction between the protein and the solid phase;
- (3) structural rearrangement of the protein upon adsorption;
- (4) and rearrangement of the excluded water or ion molecules in bulk solution.

Taking this into consideration, possible explanations for the first and second endothermic heat signals are sub-processes (1), (3) and (4). This hypothesis is supported with previous studies: Dehydration process, i. e., the partial removal of water molecules from protein groups, was determined to be endothermic^{18,39}. Protein conformational changes and repulsive forces between same charges or between hydrophilic moieties and hydrophobic groups were reported to also have an endothermic nature^{29,37,50}.

The possibility of BSA aggregates formation and adsorption was also considered in the microcalorimetric results analysis. However, it has been reported that monomeric BSA form exceeds 85% at basic pH values⁴¹. Having its isoelectric point between 4.8 to 5.6⁴¹, at pH 9 the protein is in a highly charged state. When proteins are charged, the repulsive effects between them will increase and lower dimerization⁴¹. Therefore, at these working conditions the monomer-dimer equilibrium in solution is likely to be displaced to the monomer state, supporting the idea that dimer adsorption does not significantly contribute to the resulting thermogram peaks.

4.3.1 First endothermic peak

Due to Yamamoto model and the endothermic nature of the removal of water molecules and ions, more thoroughly mentioned in subchapter 1.6 of this work, we were led to believe that the first endothermic peak may be due to dehydration related processes (1) and (4). It should be taken into consideration that these sub-processes are related and very often overlap in time. Coupled with this, the results shown in Figure 20 indicate that protein surface concentration strongly correlates with the total area of the first endothermic peak. Given that there is a higher amount of molecules adsorbing, there should be a higher dehydration and ion release from both protein and resin, leading to higher energies necessary to remove them^{18,29}.

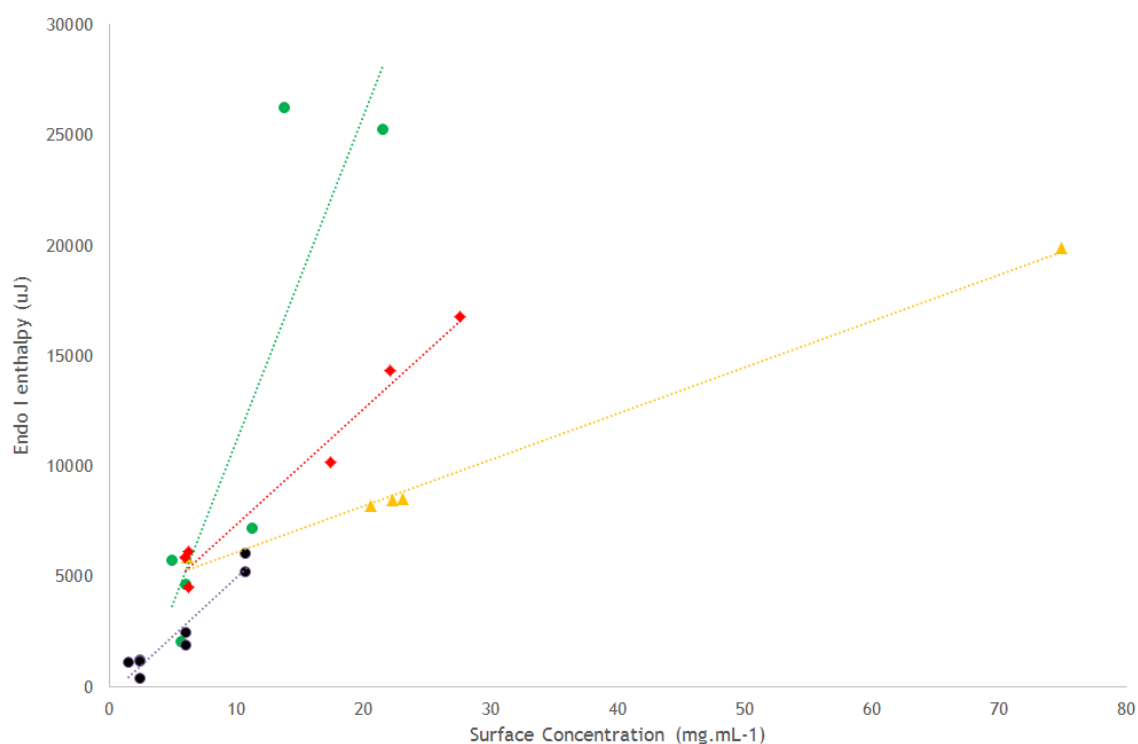


Figure 20 - First endothermic peak area related with surface concentration obtained for 230 µL injections of BSA in Tris-HCl pH 9 adsorbing onto (●) TSKgel SuperQ 5PW, (◆) Toyopearl DEAE 650M and (▲) Toyopearl GigaCap Q-650M. First endothermic peaks obtained for 30 µL injections of the same solutions onto (●) TSKgel SuperQ 5PW are also shown. Only considered trials with a linear relation between injection concentration and surface concentration were considered.

It is important to refer that for the specific case of TSKgel SuperQ, flowthrough values (protein that did not adsorb divided by input total protein) in the range of 80% were observed when injecting 230 μL . In other words, it was noticed that a high amount of proteins were flowing through TSKgel SuperQ without adsorbing, even though the experiments were done below the resin's maximum capacity. Several factors may be involved, like incomplete titration of ligands upon equilibrium [Ales], but we believe that the main reason for this difference is due to the age of the TSKgel SuperQ available on the laboratory (approximately 15 years). This could compromise the available ligands in this support, hence lowering the binding capacity and, consequently, explains the very high flowthrough values observed. In order to have a better understanding of what was happening, other experiments were done injecting 30 μL of BSA solutions in TSKgel SuperQ. These experiments did not present any flowthrough.

All things considered, since TSKgel SuperQ trials with 30 μL injections did not reached the diminished resin maximum capacity (due to no observed flowthrough), we believe that the results obtained with the lower volume loop represents more accurately the energies involved in the inherited mechanism of BSA adsorption onto TSKgel SuperQ. Henceforward, these results will be presented in the interpretation of the following thermodynamic events.

Looking again to TSKgel SuperQ endothermic areas shown in Figure 20, and considering what has been discussed previously, the results obtained for 30 μL injections were more expected than the results obtained using 230 μL injections. Since they show that TSKgel SuperQ present more similar dehydration energies with the other grafted resin, Toyopearl GigaCap.

Toyopearl GigaCap and TSKgel SuperQ, although bearing a higher charged ligand than Toyopearl DEAE at this pH, show a lower dehydration heat when compared with Toyopearl DEAE. Our hypothesis is that this could be due to the fact that they bear grafted ligands with a tree-like tridimensional disposition (shown in the schematics of table X). Toyopearl DEAE has a two dimensional disposition of the ligands and this could mean the presence of a higher number of ordered water molecules and ions. Therefore the energy requirement to remove these organized water molecules and counter-ions is higher.

As explained in chapter one, it is important to note that although dehydration process is endothermic, it is considered a spontaneous process because it is compensated by the entropy gain resulting from the release water molecules and ions^{29,40}.

4.3.2 Second endothermic peak

The second endothermic peak seems to have, as well, a close relation to surface concentration (Figure 21). This occurs at the same time or shortly after dehydration. Increasing surface concentration causes an increase of the area of the second endothermic event, which could indicate the repulsion between already adsorbed molecules, molecule re-orientation, and/or conformational alterations. Other previous studies suggest that these processes have an endothermic nature ^{37,56}. In addition, it was found that BSA undergoes structural rearrangements upon adsorption ⁷⁶ and these appear to be greater in the absence of salt ⁷⁷.

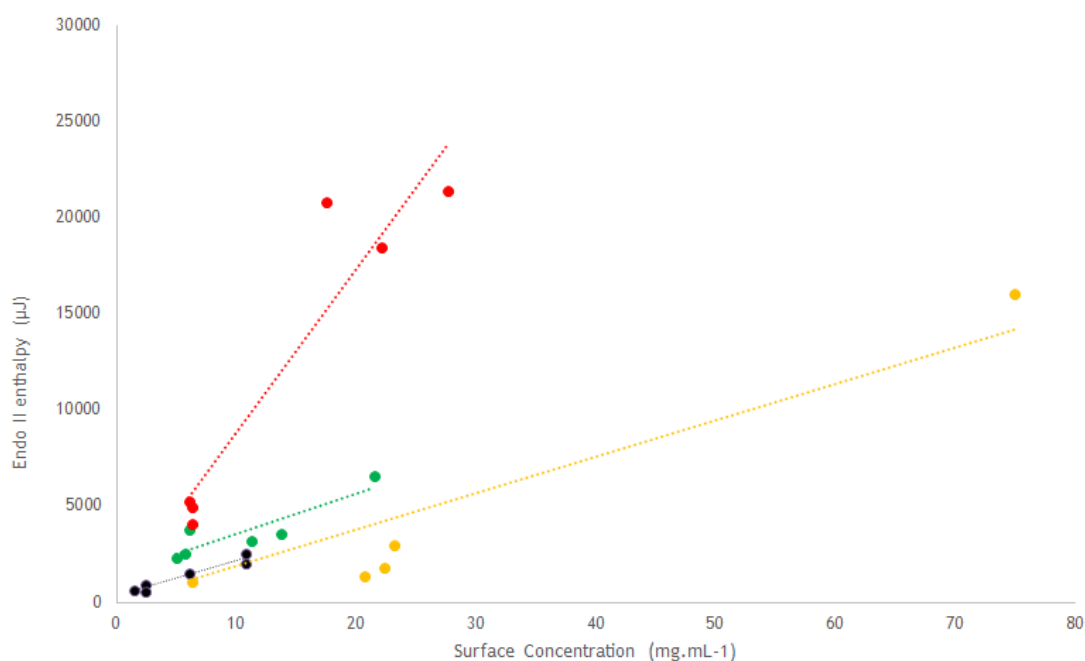


Figure 21 - Second endothermic peak area related with surface concentration obtained for 230 μL injections of BSA in Tris-HCl pH 9 adsorbing onto (●) TSKgel SuperQ 5PW, (◆) Toyopearl DEAE 650M and (▲) Toyopearl GigaCap Q-650M. Second endothermic peaks obtained for 30 μL injections of the same solutions onto (●) TSKgel SuperQ 5PW are also shown. Only considered trials with a linear relation between injection concentration and surface concentration were considered.

Notably, Toyopearl DEAE has in average higher second endothermic signals, followed by TSKgel SuperQ and finally Toyopearl GigaCap. Our hypothesis is that in DEAE, due to the ligands being directly attached to the solid phase, BSA repulsion is higher than in the other supports where the ligands could be more spatially apart. Due to increasing protein loading on resin surface, protein-protein interactions may become increasingly dominant and create a different free energy minimum state to which proteins adapt ⁴⁰. It is assumed that proteins initially adapt to a conformation that maximizes surface-protein interaction resulting from electrostatic attraction. However, this may become unfavorable in higher surface concentrations due to repulsion between same-charged patches facing each other ⁴⁰. This repulsion can obviously be one of the sources of neighboring protein conformational alterations. Equally important, last generation supports Toyopearl GigaCap and TSKgel SuperQ

have the lowest second endothermic peaks. Due to the same reasons stated before, the grafting and 3D disposition of ligands seem to lower protein conformational alterations when comparing to Toyopearl DEAE. In summary, the 2D ligand disposition in Toyopearl DEAE induces a higher footprint (higher spreading) of BSA upon adsorption. In grafted resins, the “soft” protein it is more likely to end-up with a conformation closer to its globular form.

4.3.3 Exothermic peak

Concerning the exothermic peak, our hypothesis based on prior studies ^{2,29,31} is that the exothermic peak may comprise processes with different natures: protein desorption; surface transport; secondary adsorption; and solution protein interaction with already adsorbed proteins.

Adsorbed protein-protein repulsive forces may induce transitions in protein local structure, such as hydrophobic groups’ exposure or alteration of the charge distribution ². This repulsive forces may also be responsible for BSA re-orientation/conformational alteration at the chromatographic surface changing the amount of binding points between the resin and protein, and consequently altering its binding strength in the process ^{2,29,48}. Adsorbed BSA binding strength alteration can lead to surface transport and even protein desorption. This is supported by Figure 22 that correlates the exothermic peak area with the percentage of protein that flowed through the support in the equilibration step. Please note the interesting fact that when the protein flowthrough is lower than 10%; the exothermic peak area is very low, especially in Toyopearl GigaCap, in which is absent.

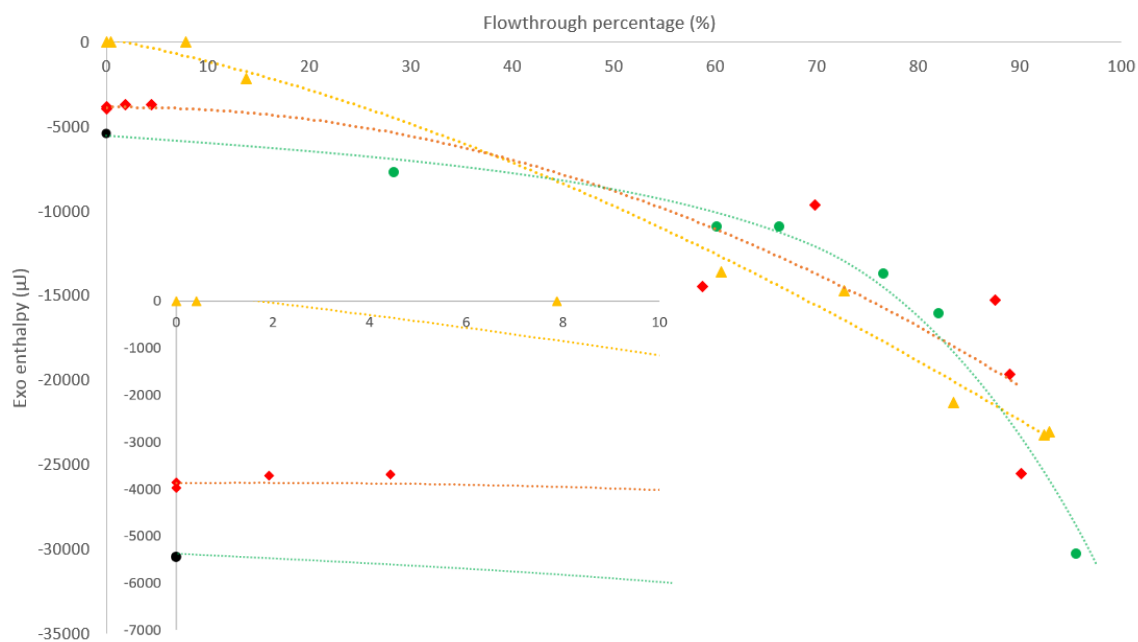


Figure 22 - Exothermic peak area related with flowthrough obtained for 230 μL injections of BSA in Tris-HCl pH 9 adsorbing onto (●) TSKgel SuperQ 5PW, (◆) Toyopearl DEAE 650M and (▲) Toyopearl GigaCap Q-650M. Note that TSKgel SuperQ 5PW thermogram with no flowthrough (●) was obtained with a 30 μL loop. The smaller graph in the left bottom corner is a zoom in of lower flowthrough percentages.

Another explanation for the exothermic event is the presence of surface transport mechanisms, supported by the trials where no flowthrough was observed. Activated jump (Figure 23 - Top) is a surface transport mechanism present in all resins, and consists in the protein hopping under adsorbed state without desorption and re-adsorption². Other transport mechanism, named chain delivery (Figure 23 - Bottom), may also be present in higher generation grafted resins Toyopearl GigaCap and TSKgel SuperQ. This is very well explained by Yu and co-workers² and consists in the delivery of an adsorbed molecule from a flexible grafted chain to a close enough neighboring chain. These surface transport mechanisms are highly related with maximum binding capacity (q_{max}) and affinity constant (K_A) values². Due to the charged ligands, both surface transport mechanisms possibly involve electrostatic interactions, which, like the presented data, were found to have mainly exothermic nature^{31,39}.

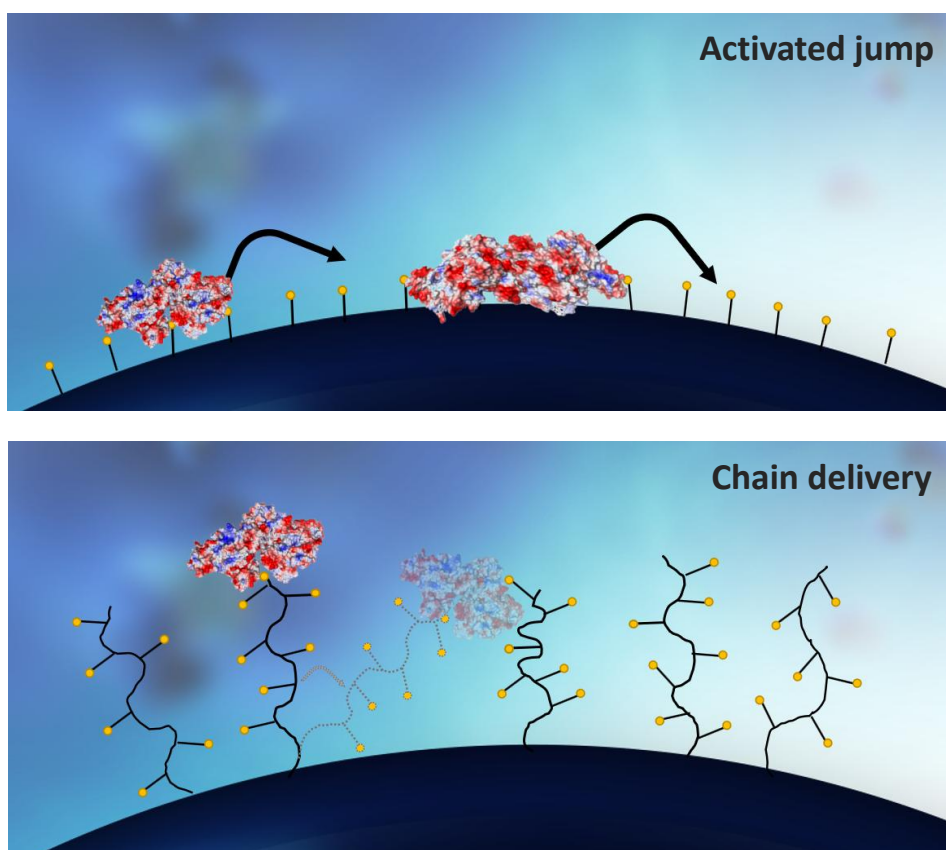


Figure 23 - Schematics of surface transport mechanisms present in IEC resins. (Top) Activated jump present in all IEC resins and (Bottom) Chain delivery mechanism present in grafted resins, for example: TSKgel SuperQ and Toyopearl GigaCap. Adapted from²

As previously explained, when injecting 30ul of BSA solution onto TSKgel SuperQ no flowthrough was observed, even though an exothermic peak was present. This further suggests that surface transport mechanisms are present. Another observation that supports this hypothesis is that a correlation between surface concentration and the exothermic peak area was found (Figure 24).

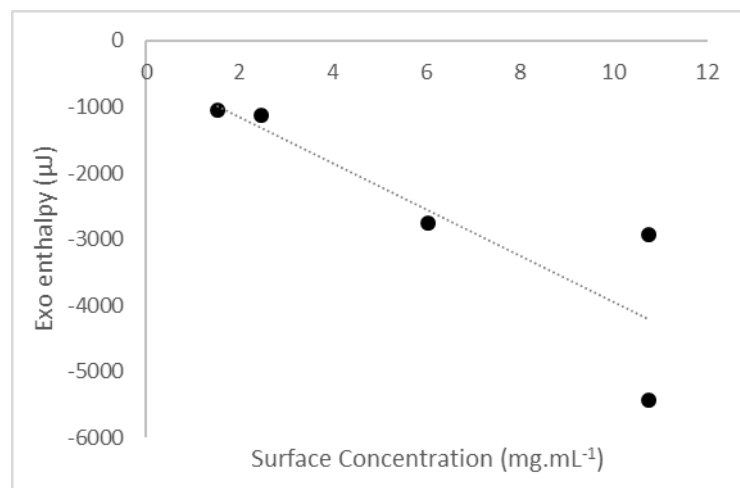


Figure 24 - Exothermic peak area related with surface concentration obtained with 30 μL injections of BSA in Tris-HCl pH 9 adsorbing onto TSKgel SuperQ 5PW. Obtained with no flowthrough.

The possibility of solution protein interaction with already adsorbed proteins was also considered, due to its observation in prior thermodynamic plasmid DNA adsorption studies under volume overloading working conditions ³¹. However, since we are operating in the linear zone of the adsorption isotherm and all exothermic peaks maximum occur on average 500 seconds later than the end of plug, the exothermic events take place in absence of BSA molecules in the flowing solution. This leads us to believe that solution protein interaction with adsorbed protein was not a major contribution.

4.3.4 “Non-binding” conditions data

BSA adsorption onto TSKgel SP 5PW at pH 9, considered an interaction under “non-binding conditions” also referred by some authors^{28,78} to as “adsorption on the wrong side”, completely changes the thermogram profile as we can see in Figure 25. Adsorption of a net negative protein onto a like-charged surface has already been observed^{37,40} and has been explained by the protein heterogeneous surface and its capacity for structural rearrangements⁴⁰. Proteins adsorbing at positively or negatively charged surfaces tend to expose oppositely charged regions independently of their net charge^{28,40}. This phenomena, called “protein charge regulation” is particularly visible for soft proteins like BSA^{78,79}.

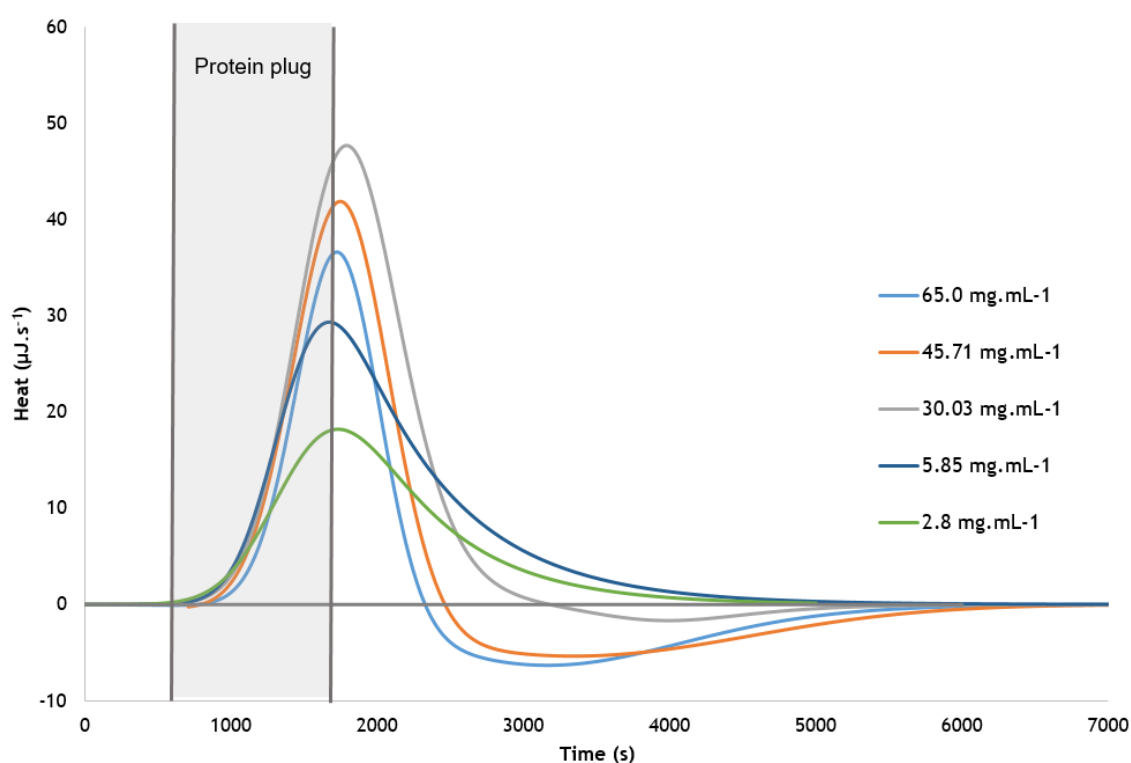


Figure 25 - FMC thermograms obtained for 230 μL injection of different concentrations of negatively net charged BSA in equilibrium buffer Tris-HCl pH 9 adsorbing onto negatively charged TSKgel SP 5PW. Surface concentrations are respectively (green) 2.8 mg.mL^{-1} , (dark blue) 5.85 mg.mL^{-1} , (grey) 30.03 mg.mL^{-1} , (orange) 45.71 mg.mL^{-1} and (light blue) 65.0 mg.mL^{-1} . Shaded area represents the interval of time at which there was protein flowing through the cell.

Under these non-binding conditions, it was observed a very high exothermic event followed, only at higher surface concentrations, by an endothermic one (Figure 25). In these cases, the thermograms were deconvoluted into two peaks (one exothermic and one endothermic). It can be seen, in Figure 26, that the exothermic peak area increases (resulting in more negative enthalpy) as surface concentration increases until the supports static maximum binding capacity is reached ($13.8 \pm 2.4 \text{ mg.mL}^{-1}$, obtained from the application of the Langmuir model to isotherm data presented in Table 8). It can also be observed (Figure 25) that when the protein plug stops its contact with the adsorbent, the exothermic event starts

decreasing. As mentioned in subchapter 1.4, different types of interaction may be involved in this exothermic behavior. Our hypothesis is that electrostatic attractive interactions between the support and protein^{28,37,40} justify the observed highly exothermic heat (around -43 mJ).

Of course, protein conformation alteration and the de-counter-ion involved in the process comprises endothermic heats^{18,37,50}, nevertheless these are overcome by the pure electrostatic attraction. When the protein is forced to interact with the support, when in the vicinity of the ligand brush, it changes its conformation promoting a highly energetic interaction as the one observed in the present study^{28,78}.

Adsorption based on hydrophobic interaction was also considered, however in our particular case the enthalpy was found to be highly exothermic (not compatible with the energy release for a hydrophobic interaction), reinforcing our belief that electrostatic contributions play a major role. It was also thought that van der Waals forces could be involved, but this hypothesis was discarded due to finding that van der Waals forces in the absence of salt are not very significant³⁶.

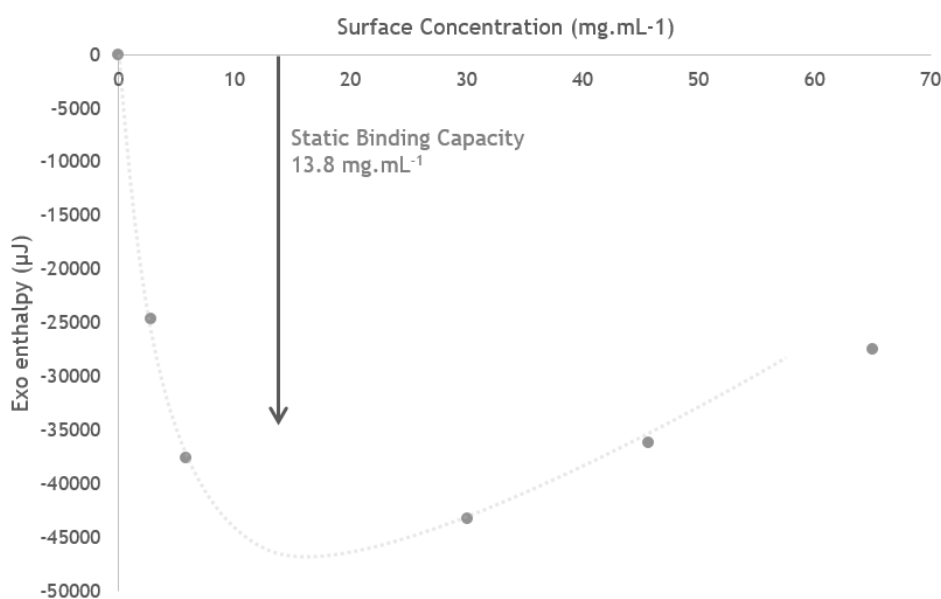


Figure 26 - Exothermic peak area related with BSA surface concentration. Obtained with TSKgel SP 5PW with 230 μ L injections with Tris HCl pH 9.

Interestingly, for surface concentrations above the adsorption isotherm “plateau zone”, an endothermic peak appears. The endothermic part of the thermogram seems to comprise adsorbed protein-protein repulsive events present at higher surface concentration. As the monolayer is being completed, repulsion between adsorbed proteins increases^{29,59}.

Adsorption “on the wrong side” was found to be highly dependent on salt concentration in previous studies^{28,78}. These studies, conducted with negatively charged brush layer (made of poly-acrylic acid), observed that maximum adsorption is found near the point of zero charge of the protein. However, substantial adsorption was observed where negatively charged BSA

adsorbed onto the negatively charged brush layer, up to a specific pH value (which the authors named *critical pH*). *Critical pH* is highly depended on salt concentration. Thus, some preliminary trials were conducted with TSKgel SP in the presence of 50 mM NaCl pH 9 (also negatively net charged protein and negative charged ligand conditions). Remarkably, as seen in Figure 27, the thermogram profile with the use of salt is completely different when compared with the ones obtained with the same resin in the absence of salt (Figure 25). It can be seen an endothermic event followed by an exothermic one. As the reader may recall, this behavior was found in the interaction of negatively charged BSA with positively charged resins (TSKgel SuperQ, Toyopearl DEAE and Toyopearl GigaCap). In other words, the presence of salt in non-binding conditions inverts the thermogram behavior back to the profile observed when ion exchange conducts the adsorption process.

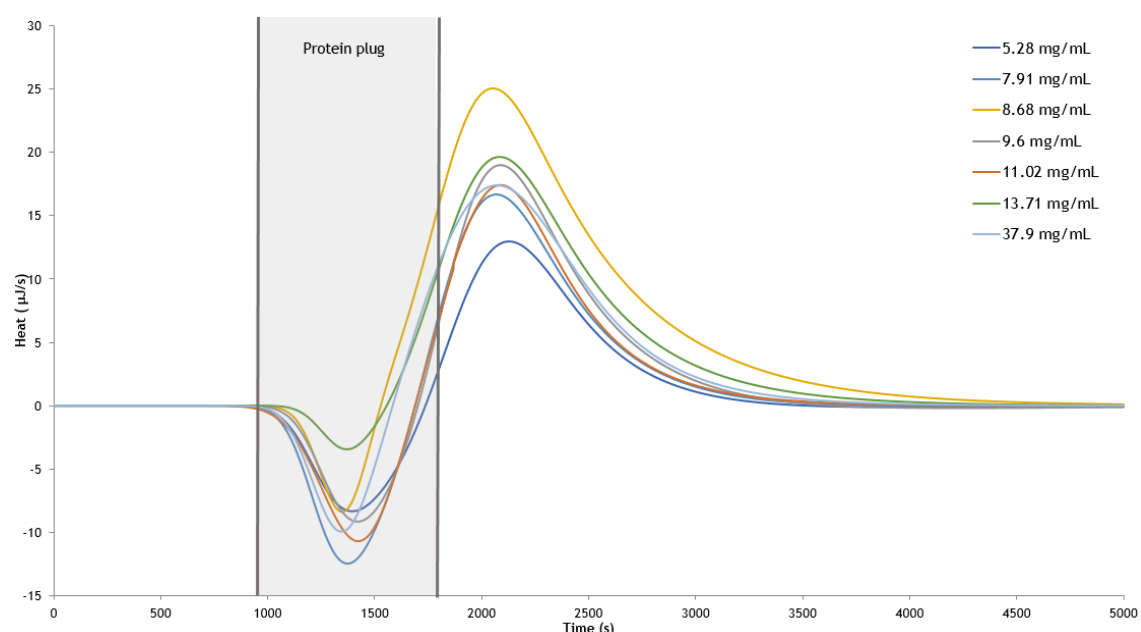


Figure 27 - FMC thermograms obtained for 230 μL injection of BSA in 20 mM Tris-Hcl at pH 9 with 50 mM NaCl adsorbing onto TSKgel SP 5PW with the respective surface concentration obtained. The shaded area corresponds to the protein plug in the cell.

As already stated before, endothermic peaks were connected several times with the release of water molecules and counter-ions^{29,31,37}. Theoretical calculations indicate that the main driving force of adsorption in “non-binding” conditions in the presence of salt is the release of counter-ions, which is related to the existence of distinct positively and negatively charged patches on the protein surface (Figure 4). As long as a protein molecule has patches of sufficient size, like BSA, the counter-ions will form a chain and will associate with oppositely charged patches and will evade similarly charged patches. This associations of the counter-ions chains with the oppositely charged patches release counter-ions, hence the appearance of the endothermic peak. This will lead to an increase in entropy of the system driving the adsorption process. This explanation may justify the observed inversion in the thermogram profile when in presence of salt.

Adsorption was reduced while working with salt, as can be seen in the isotherm (Figure 28), because the maximum pH until “non-binding conditions” is observed (*critical pH*) decreases⁷⁸. Also, it was observed that protein flowthrough in presence of salt is around 94% whereas in its absence is around 77%.

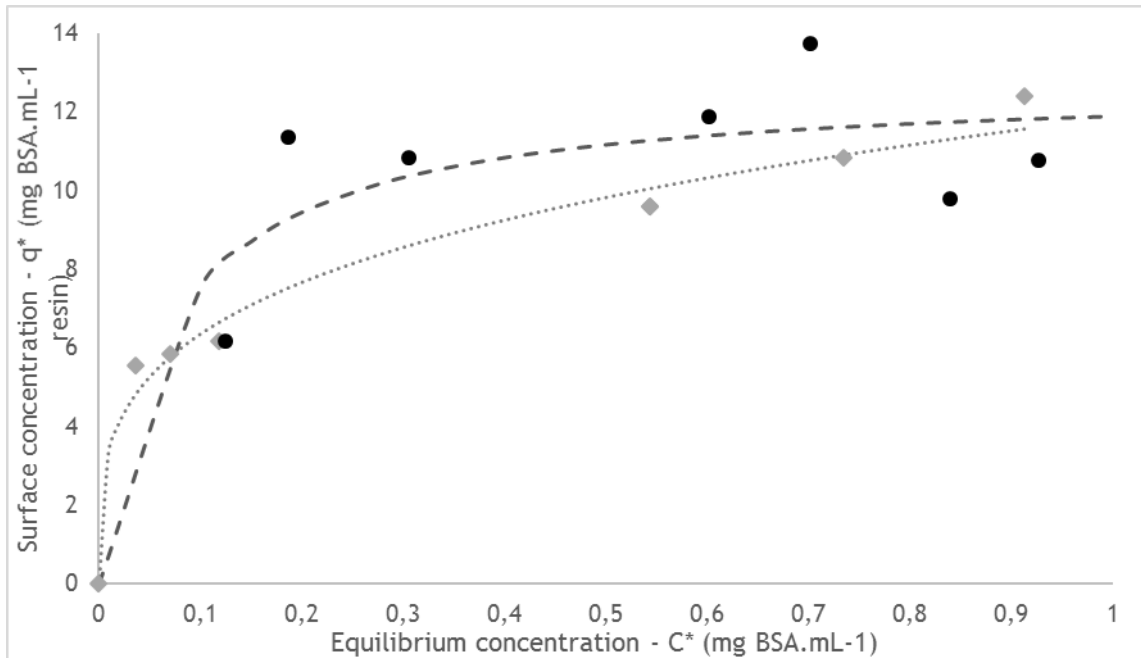


Figure 28 - Equilibrium binding isotherm for BSA adsorption onto TSKgel SP 5PW in Tris-HCl pH 9 with 20 mM Tris at 295 K in the absence of salt (●) and with 50 mM NaCl (◆).

4.4 Adsorption driving forces

Regarding the driving forces of adsorption, two moments could be considered, signal obtained during the contact of the protein plug with the adsorbent and signal obtained after the plug leaves the cell. For the analyzed anion-exchangers it is important to note that while protein solution is passing through the cell (before $t = 1680s$, time when the mobile phase plug containing BSA is replaced by BSA-free mobile phase), the net heat of adsorption is endothermic (see Figure 18). Paying closer attention to equation 1 in sub-chapter 1.7, for a process to spontaneously occur ΔG° needs to be negative. If the adsorption process is dominated by endothermic energy (positive values for ΔH°) the entropic effects are considered to dominate the adsorption process. The adsorption process occurs due to large entropy gains that compensates that enthalpically unfavorable condition. In other words, the enthalpic energy requirement is later compensated by the higher water molecule and ions degrees of freedom gained, also known as, entropy gains. This entropic driving force was observed, as already mentioned, for the studied anion exchangers, TSKgel SuperQ, Toyopearl GigaCap and Toyopearl DEAE, and for the cation exchanger TSKgel SP in presence of 50 mM NaCl. On the other hand, in TSKgel SP, adsorption heat is negative in the absence of salt (Figure 25), meaning that in this case adsorption is enthalpically driven.

Taking all this information into account, it is of utmost importance to refer that the existence of exothermic signals (anion exchanger in the present study) and endothermic signals (cation exchanger in the present study) after the protein plug is also considered an important part of the overall protein adsorption mechanism. These latter phenomena, i.e. protein-protein repulsion, protein desorption, conformational alterations, binding strength alteration, and surface transport mechanisms, should be considered as an integral part of the process and therefore considered in the development of future stationary phases, molecular simulations and experimental investigations.

Chapter 5 - Conclusions

Considering that energy changes from different sources are involved in the adsorption process, microcalorimetry displayed once more the capability of a valuable insight on the overall process.

With a negative net charge, BSA adsorption was studied onto:

- Anion exchanger TSKgel SuperQ 5PW at pH 9 in the absence of salt;
- Cation exchanger TSKgel SP 5PW in absence and presence of sodium chloride (50 mM).

It was seen that, in the absence of salt, TSKgel SuperQ 5PW showed the same thermogram behavior than other commercial anion exchangers (Toyopearl DEAE and Toyopearl GigaCap), presenting an endothermic part that was deconvoluted into two endothermic signals followed by a single exothermic signal. Although the thermogram behavior was similar, the intensity, area, and shape of the peaks varied relatively between resins.

The derived observations and conclusions were developed within the mechanistic framework proposed by Yamamoto and co-workers. The first peak, endothermic, increased with protein surface concentration and was considered to be connected to:

- Water molecules and ion release from the protein and support;
- Rearrangement of the excluded ions or water molecules in the solution.

A close relation was also found between the second endothermic peak and surface concentration. That fact together with its timing led to the conclusion that this peak comprised:

- Protein-protein repulsion;
- Conformational alterations;
- Molecule re-orientation.

Lastly, exothermic peak showed a correlation between protein flowthrough and surface concentration when injection concentrations were low. It was found to be related to:

- Protein desorption (at high injection concentrations);
- Secondary adsorption (at high injection concentrations).
- Surface transport mechanisms - activated jump and chain delivery (when injection concentrations were low);

Interestingly, surface transport mechanisms were never mentioned in prior ITC or other static adsorption study techniques. This could be due to the fact that these mechanisms are intensified in flow conditions. The use of flow microcalorimetry enabled this possible observation. This protein hopping between ligands inside a chromatographic column can lead

to desorption, making the protein leak even in the equilibrium step at higher injected concentrations.

Another important finding to note, is the change in thermogram profile in a same-charged protein-resin system. And when in presence of 50 mM NaCl, its inversion back to the profile observed while ion exchange mechanisms drive the adsorption process. Adsorption of a net negative protein onto a like-charged surface in absence of salt, has been previously observed^{13,28,37} and explained by “protein charge regulation”. This behavior was found to be suppressed in presence of salt leading to the return of the interaction mechanism to its original for an ion exchange interaction and consequently to the inversion of the FMC profile.

For future work, further experiments should be conducted with the studied anion exchangers. This time, in the presence of salt, due to its known effects in ion exchange chromatography, expecting to observe the existence of differences in the shape and magnitude of the thermograms. In addition, it would be very interesting to conduct further comparative experimental studies using resins with “gel-in-a-shell” and “salt-tolerance” features.

Ultimately, the author hopes to have shed some light on the complexity of protein adsorption and the important role of: protein-protein interactions on the adsorbent surface, protein reorientation and/or conformation change, surface transport mechanisms, and protein and adsorbent surface dehydration in the establishment of the adsorptive process. Theoretical, empirical models and future computational simulations of adsorption equilibrium should account for these complex effects, as well as the primary interactions. Because of the direct correlation between heat of adsorption data and these non-specific interactions, it would certainly be advantageous to use calorimetry data in model selection or development. The use of such data also provides valuable insight regarding the underlying driving forces for protein adsorption.

References

1. Parris, N. A. *Instrumental Liquid Chromatography: A Practical Manual on High-Performance Liquid Chromatographic Methods*. (Elsevier, 2000). at <<https://books.google.com/books?id=NAKUalcZ78QC&pgis=1>>
2. Yu, L., Zhang, L. & Sun, Y. Protein behavior at surfaces: Orientation, conformational transitions and transport. *J. Chromatogr. A* **1382**, 118-134 (2015).
3. Leader, B., Baca, Q. J. & Golan, D. E. Protein therapeutics: a summary and pharmacological classification. *Nat. Rev. Drug Discov.* **7**, 21-39 (2008).
4. Keen, H. *et al.* Human Insulin Produced By Recombinant Dna Technology: Safety and Hypoglycæmic Potency in Healthy Men. *Lancet* **316**, 398-401 (1980).
5. Nature Journal official definition. at <<http://www.nature.com/subjects/recombinant-protein-therapy>>
6. Carta, G. & Jungbauer, A. *Protein chromatography process development and scale-up*. (WILEY-VCH, 2010).
7. Marston, A., Hostettmann, M. & Hostettmann, K. *Preparative Chromatography Techniques*. (Springer-Verlag, 1986).
8. Cherry, J. P. *Methods for Protein Analysis*. (The American Oil Chemists Society, 1988). at <<https://books.google.com/books?id=bLGOH3m59JcC&pgis=1>>
9. Alberts, B. *et al.* *Analyzing Protein Structure and Function*. (Garland Science, 2002). at <<http://www.ncbi.nlm.nih.gov/books/NBK26820/>>
10. Huang, J., Wang, F., Ye, M. & Zou, H. Enrichment and separation techniques for large-scale proteomics analysis of the protein post-translational modifications. *J. Chromatogr. A* **1372C**, 1-17 (2014).
11. Matsuda, R., Anguizola, J., Joseph, K. S. & Hage, D. S. Analysis of drug interactions with modified proteins by high-performance affinity chromatography: Binding of glibenclamide to normal and glycated human serum albumin. *J. Chromatogr. A* **1265**, 114-122 (2012).
12. Kastner, M. *Protein Liquid Chromatography*. (Elsevier B.V., 2000).
13. Müller, E. Properties and Characterization of High Capacity Resins for Biochromatography. *Chem. Eng. Technol.* **28**, 1295-1305 (2005).
14. Lenhoff, A. M. Protein adsorption and transport in polymer-functionalized ion-exchangers. *J. Chromatogr. A* **1218**, 8748-8759 (2011).
15. Moo-Young, M. *Comprehensive Biotechnology*. (Newnes, 2011). at <<http://dx.doi.org/10.1002/9783527627646.ch11>>
16. Reach Devices website. at <<http://www.reachdevices.com/Protein/ProteinPurification.html>>
17. Schrödinger. PyMol - Educational Version 1.7.4. (2016). at <<https://www.pymol.org/>>

18. Lin, F., Chen, W. & Hearn, M. T. W. Thermodynamic analysis of the interaction between proteins and solid surfaces : application to liquid chromatography. *J. Mol. Recognit.* **15**, 55-93 (2002).
19. Liang, J., Fieg, G. & Jakobtorweihen, S. Molecular Dynamics Simulations of a Binary Protein Mixture Adsorption onto Ion-Exchange Adsorbent. *Ind. Eng. Chem. Res.* **54**, 2794-2802 (2015).
20. Xie, Y., Liao, C. & Zhou, J. Effects of external electric fields on lysozyme adsorption by molecular dynamics simulations. *Biophys. Chem.* **179**, 26-34 (2013).
21. Liang, J. & Fieg, G. A combination of experiments and molecular dynamics simulation for the investigation of the ion-exchange adsorption of biological macromolecules. *Comput. Aided Chem. Eng.* **1**, 25-30 (2013).
22. Latour, R. Molecular Simulation Methods to Investigate Protein Adsorption Behavior at the Atomic Level. *Compr. Biomater.* **1**, 171-192 (2011).
23. Gundersen, S. I. & Palmer, A. F. Conjugation of Methoxypolyethylene Glycol to the Surface of Bovine Red Blood Cells. *Biotechnol. Bioeng.* **96**, 1199-1210 (2007).
24. Euston, S. R. Computer simulation of proteins: adsorption, gelation and self-association. *Curr. Opin. Colloid Interface Sci.* **9**, 321-327 (2004).
25. Delgado-Magnero, K. H., Valiente, P. A., Ruiz-Peña, M., Pérez-Gramatges, A. & Pons, T. Unraveling the binding mechanism of polyoxyethylene sorbitan esters with bovine serum albumin: A novel theoretical model based on molecular dynamic simulations. *Colloids Surfaces B Biointerfaces* **116**, 720-726 (2014).
26. Chen, M., Zheng, T., Wu, C. & Xing, C. Molecular dynamics simulations of collagen adsorption onto grooved rutile surface: the effects of groove width. *Colloids Surf. B. Biointerfaces* **121**, 150-7 (2014).
27. Talbot, J., Tarjus, G., Van Tassel, P. R. & Viot, P. From car parking to protein adsorption: An overview of sequential adsorption processes. *Colloids Surfaces A Physicochem. Eng. Asp.* **165**, 287-324 (2000).
28. De Vos, W. M., Leermakers, F. A. M., De Keizer, A., Stuart, M. A. C. & Kleijn, J. M. Field theoretical analysis of driving forces for the uptake of proteins by like-charged polyelectrolyte brushes: Effects of charge regulation and patchiness. *Langmuir* **26**, 249-259 (2010).
29. Silva, G. L., Marques, F. S., Thrash, M. E. & Dias-Cabral, A. C. Enthalpy contributions to adsorption of highly charged lysozyme onto a cation-exchanger under linear and overloaded conditions. *J. Chromatogr. A* **1352**, 46-54 (2014).
30. Jachimska, B. & Pajor, A. Physico-chemical characterization of bovine serum albumin in solution and as deposited on surfaces. *Bioelectrochemistry* **87**, 138-146 (2012).
31. Aguilar, P., Twarda, A., Sousa, F. & Dias-Cabral, A. C. Thermodynamic study of the interaction between linear plasmid deoxyribonucleic acid and an anion exchange support under linear and overloaded conditions. *J. Chromatogr. A* **1372**, 166-173 (2014).

32. Norde, W. Driving forces for protein adsorption at solid surfaces. *Macromol. Symp.* **103**, 5-18 (1996).
33. High definition image library. at
<<http://hdimagelib.com/hydrogen+bond?image=418661904>>
34. Bianco, V., Iskrov, S. & Franzese, G. Understanding the role of hydrogen bonds in water dynamics and protein stability. *J. Biol. Phys.* **38**, 27-48 (2012).
35. Mirani, M. R. & Rahimpour, F. Thermodynamic modelling of hydrophobic interaction chromatography of biomolecules in the presence of salt. *J. Chromatogr. A* **1422**, 170-177 (2015).
36. Kim, J., Desch, R. J., Thiel, S. W., Gulians, V. V & Pinto, N. G. Energetics of lysozyme adsorption on mesostructured cellular foam silica: effect of salt concentration. *J. Chromatogr. A* **1218**, 6697-704 (2011).
37. Katiyar, A., Thiel, S. W., Gulians, V. V & Pinto, N. G. Investigation of the mechanism of protein adsorption on ordered mesoporous silica using flow microcalorimetry. *J. Chromatogr. A* **1217**, 1583-8 (2010).
38. Huang, H., Lin, F., Chen, W. & Ruaan, R. Isothermal Titration Microcalorimetric Studies of the Effect of Temperature on Hydrophobic Interaction between Proteins and Hydrophobic Adsorbents. *J. Colloid Interface Sci.* **229**, 600-606 (2000).
39. Ross, P. D. & Subramanian, S. Thermodynamics of protein association reactions: forces contributing to stability. *Biochemistry* **20**, 3096-3102 (1981).
40. Rabe, M., Verdes, D. & Seeger, S. Understanding protein adsorption phenomena at solid surfaces. *Adv. Colloid Interface Sci.* **162**, 87-106 (2011).
41. Barbosa, L. R. S. *et al.* The importance of protein-protein interactions on the pH-induced conformational changes of bovine serum albumin: A small-angle x-ray scattering study. *Biophys. J.* **98**, 147-157 (2010).
42. Lin, F., Chen, C., Chen, W. & Yamamoto, S. Microcalorimetric studies of the interaction mechanisms between proteins and Q-Sepharose at pH near the isoelectric point (pI): Effects of NaCl concentration, pH value, and temperature. *J. Chromatogr. A* **912**, 281-289 (2001).
43. Lin, F. Y., Chen, W. Y., Ruaan, R. C. & Huang, H. M. Microcalorimetric studies of interactions between protein and hydrophobic ligands in hydrophobic interaction chromatography: effects of ligand chain length, density, and the amount of bound protein. *Prog. Biotechnol.* **16**, 59-62 (2000).
44. Ee, J. I. W. U. L. Microcalorimetric Studies of the Interactions of Imidazole with Immobilized Cu (II): Effects of pH Value and Salt Concentration. *J. Colloid Interface Sci.* **242**, 236-241 (1996).
45. Ee, J. I. W. U. L. Microcalorimetric Studies of the Interactions of Lysozyme with Immobilized Cu(II) : Effects of pH Value and Salt Concentration. *J. Colloid Interface Sci.* **242**, 49-54 (1996).
46. Huang, H., Lin, F., Chen, W. & Ruaan, R. Isothermal Titration Microcalorimetric

- Studies of the Effect of Temperature on Hydrophobic Interaction between Proteins and Hydrophobic Adsorbents. *J. Colloid Interface Sci.* **229**, 600-606 (2000).
47. Lu, D. R. & Park, K. Effect of surface hydrophobicity on the conformational changes of adsorbed fibrinogen. *J. Colloid Interface Sci.* **144**, 271-281 (1991).
 48. Marques, F. S., Silva, G. L., Thrash, M. E. & Dias-Cabral, A. C. Lysozyme adsorption onto a cation-exchanger: mechanism of interaction study based on the analysis of retention chromatographic data. *Colloids Surf. B. Biointerfaces* **122**, 801-7 (2014).
 49. Mihelic, I. Temperature influence on the dynamic binding capacity of a monolithic ion-exchange column. *J. Chromatogr. A* **987**, 159-168 (2003).
 50. Norde, W. Protein adsorption at solid surfaces: A thermodynamic approach. *Pure Appl. Chem.* **66**, 491-496 (1994).
 51. Norde, W. & Lyklema, J. Theory with Special Reference to the Adsorption of Human Plasma Albumin and Bovine Pancreas Ribonuclease at Polystyrene Surfaces. *Interface* **71**, 350-366 (1979).
 52. Dias-Cabral, A. C., Queiroz, J. A. & Pinto, N. G. Effect of salts and temperature on the adsorption of bovine serum albumin on polypropylene glycol-Sepharose under linear and overloaded chromatographic conditions. *J. Chromatogr. A* **1018**, 137-153 (2003).
 53. Deitcher, R. W., Rome, J. E., Gildea, P. A., O'Connell, J. P. & Fernandez, E. J. A new thermodynamic model describes the effects of ligand density and type, salt concentration and protein species in hydrophobic interaction chromatography. *J. Chromatogr. A* **1217**, 199-208 (2010).
 54. Connelly, P. R. *et al.* Enthalpy of hydrogen bond formation in a protein-ligand binding reaction. *Proc. Natl. Acad. Sci. U. S. A.* **91**, 1964-1968 (1994).
 55. Norde, W. Energy and Entropy of Protein Adsorption. *J. Dispers. Sci. Technol.* **13**, 363-377 (1992).
 56. Norde, W. Protein adsorption at solid surfaces: A thermodynamic approach. *Pure Appl. Chem.* **66**, 491-496 (1994).
 57. Gill, D., Roush, D., Shick, K. & Willson, R. Microcalorimetric characterization of the anion-exchange adsorption of recombinant cytochrome b5 and its surface-charge mutants. *J. Chromatogr. A* **715**, 81-93 (1995).
 58. Blaschke, T., Werner, A. & Hasse, H. Microcalorimetric study of the adsorption of native and mono-PEGylated bovine serum albumin on anion-exchangers. *J. Chromatogr. A* **1277**, 58-68 (2013).
 59. Korfhagen, J., Dias-Cabral, A. C. & Thrash, M. E. Nonspecific Effects of Ion Exchange and Hydrophobic Interaction Adsorption Processes. *Sep. Sci. Technol.* **45**, 2039-2050 (2010).
 60. Ornelas, M. *et al.* Synthesis of glycylglycine-imprinted silica microspheres through different water-in-oil emulsion techniques. *J. Chromatogr. A* **1297**, 138-45 (2013).
 61. Thrash, M. E. & Pinto, N. G. Characterization of enthalpic events in overloaded ion-exchange chromatography. *J. Chromatogr. A* **944**, 61-68 (2002).

62. Ladbury, J. & Doyle, M. *Biocalorimetry 2*. (WILEY, 2004).
63. Baker, B. M. & Murphy, K. P. Evaluation of linked protonation effects in protein binding reactions using isothermal titration calorimetry. *Biophys. J.* **71**, 2049-55 (1996).
64. Esquibel-King, M. A., Dias-Cabral, A. C., Queiroz, J. A. & Pinto, N. G. Study of hydrophobic interaction adsorption of bovine serum albumin under overloaded conditions using flow microcalorimetry. *J. Chromatogr. A* **865**, 111-122 (1999).
65. Raje, P. & Pinto, N. G. Importance of heat of adsorption in modeling protein equilibria for overloaded chromatography. *J. Chromatogr. A* **796**, 141-156 (1998).
66. Desch, R. J., Kim, J. & Thiel, S. W. Interactions between biomolecules and an iron-silica surface. *Microporous Mesoporous Mater.* **187**, 29-39 (2014).
67. Aguilar, P. Understanding the interaction between pDNA and anion exchange supports under linear and overloaded chromatographic conditions. (University of Beira Interior, 2014).
68. Langmuir, I. The Adsorption of Gases on Plane Surfaces of Glass, Mica and Platinum. *J. Am. Chem. Soc.* **40**, 1361-1403 (1918).
69. Brooks, C. & Cramer, S. Steric mass-action ion exchange: Displacement profiles and induced salt gradients. *AIChE J.* **38**, 1969-1978 (1992).
70. Roth, C. M., Sader, J. E. & Lenhoff, A. M. Electrostatic Contribution to the Energy and Entropy of Protein Adsorption. *J. Colloid Interface Sci.* **203**, 218-221 (1998).
71. Silva, G. Master's Thesis: Understanding ion-exchange adsorption mechanism under overloaded conditions. (University of Beira Interior, 2013).
72. Pousada, P. Master's Thesis: Understanding Ion Exchange adsorption mechanisms under overloaded conditions. (University of Beira Interior, 2014).
73. Tosoh Bioscience. TOSOH Ion Exchange Chromatography Catalog. (2016).
74. Bellot, J. C. & Condoret, J. S. Modelling of liquid chromatography equilibria. *Process Biochem.* **28**, 365-376 (1993).
75. Li, J., Han, W. & Yu, Y. *Chromatography Method*. (InTech, 2013).
76. Brandes, N., Welzel, P. B., Werner, C. & Kroh, L. W. Adsorption-induced conformational changes of proteins onto ceramic particles: Differential scanning calorimetry and FTIR analysis. *J. Colloid Interface Sci.* **299**, 56-69 (2006).
77. Thrash, M. E. & Pinto, N. G. Flow microcalorimetric measurements for bovine serum albumin on reversed-phase and anion-exchange supports under overloaded conditions. *J. Chromatogr. A* **908**, 293-299 (2001).
78. Vos, W. M. De, Biesheuvel, P. M., Keizer, A. De, Kleijn, J. M. & Stuart, M. A. C. Adsorption of the Protein Bovine Serum Albumin in a Planar Poly (acrylic acid) Brush Layer As Measured by Optical Reflectometry. *Langmuir* **14**, 6575-6584 (2008).
79. Vos, W. M. De, Leermakers, F. A. M., Keizer, A. De, Kleijn, J. M. & Stuart, M. A. C. Interaction of Particles with a Polydisperse Brush : A Self-Consistent-Field Analysis. *Macromolecules* **42**, 5881-5891 (2009).

Appendix I

The thermograms that were not shown in the discussion of this work whose areas were compared are shown in this appendix.

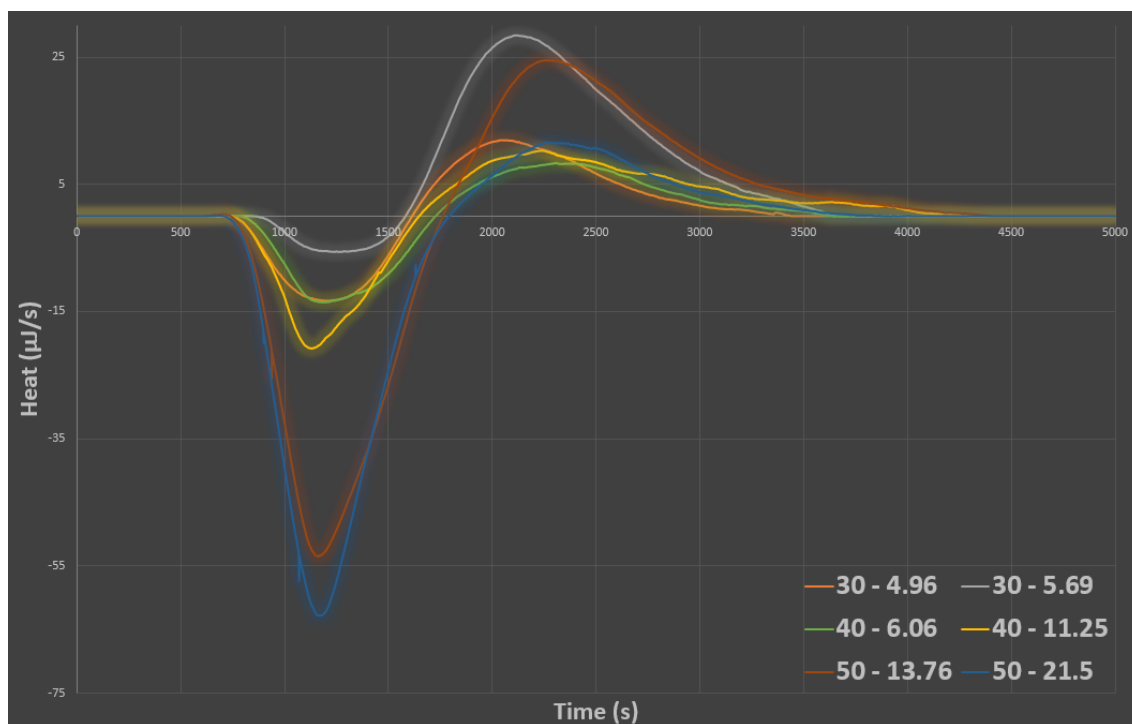


Figure 29 - FMC thermograms obtained for 230 µL injection of different BSA solutions concentrations in equilibrium buffer Tris-HCl pH 9 adsorbing onto TSKgel SuperQ 5PW. Injection concentrations are represented in the figure followed by the resulting surface concentration obtained. For example: (dark blue) thermogram was obtained injecting 50 mg.mL⁻¹ BSA solution resulting in 21.5 mg BSA.mL⁻¹ TSKgel SuperQ.

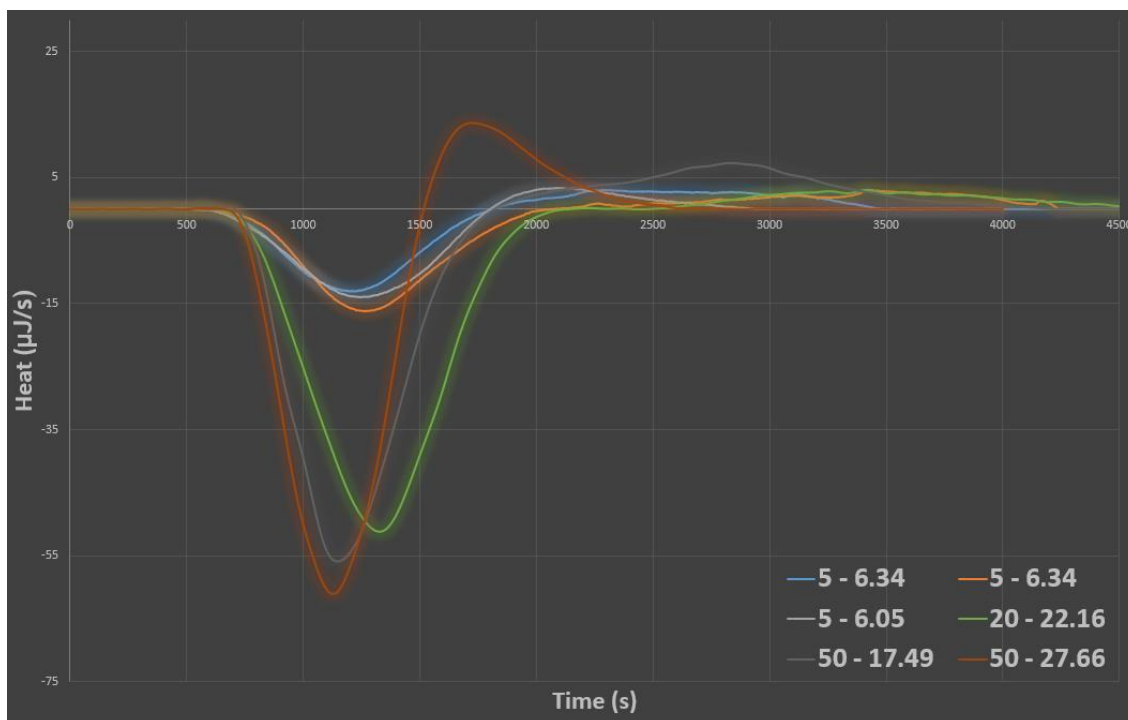


Figure 30 - FMC thermograms obtained for 230 μL injection of different BSA solutions concentrations in equilibrium buffer Tris-HCl pH 9 adsorbing onto Toyopearl DEAE 650M. Injection concentrations are represented in the figure followed by the resulting surface concentration obtained. For example: (light green) thermogram was obtained injecting 20 $\text{mg}\cdot\text{mL}^{-1}$ BSA solution resulting in 22.16 $\text{mg}\cdot\text{mL}^{-1}$ Toyopearl DEAE.

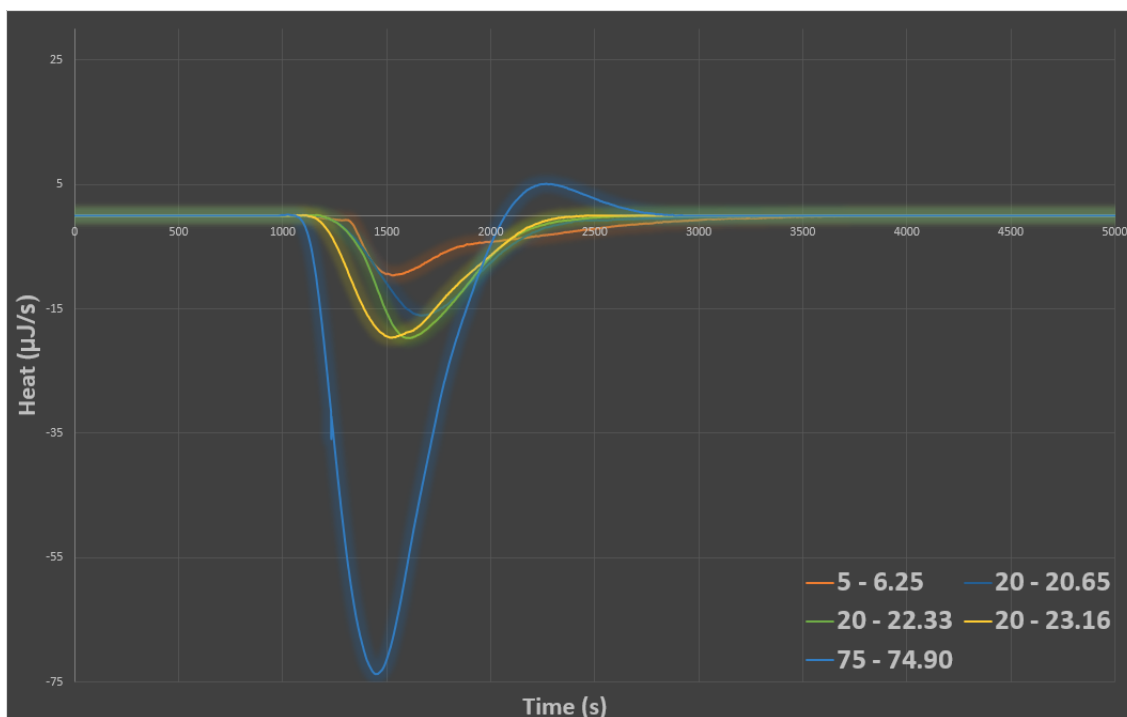


Figure 31 - FMC thermograms obtained for 230 µL injection of different BSA solutions concentrations in equilibrium buffer Tris-HCl pH 9 adsorbing onto Toyopearl GigaCap Q-650M. Injection concentrations are represented in the figure followed by the resulting surface concentration obtained. For example: (dark blue) thermogram was obtained injecting 75 mg.mL⁻¹ BSA solution resulting in 74.9 mg BSA.mL⁻¹ Toyopearl GigaCap Q-650M.